

CERN-TH/96-55
hep-ph/9604412

B Decays and CP Violation

Matthias Neubert
Theory Division, CERN, CH-1211 Geneva 23, Switzerland

Abstract

We review the status of the theory and phenomenology of heavy-quark symmetry, exclusive weak decays of B mesons, inclusive decay rates and lifetimes of b hadrons, and CP violation in B -meson decays.

(To appear in International Journal of Modern Physics A)

CERN-TH/96-55
April 1996

B DECAYS AND CP VIOLATION

MATTHIAS NEUBERT
Theory Division, CERN
CH-1211 Geneva 23, Switzerland

Received (received date)
Revised (revised date)

We review the status of the theory and phenomenology of heavy-quark symmetry, exclusive weak decays of B mesons, inclusive decay rates and lifetimes of b hadrons, and CP violation in B -meson decays.

1. Introduction

The rich phenomenology of weak decays has always been a source of information about the nature of elementary particle interactions. A long time ago, β - and μ -decay experiments revealed the structure of the effective flavour-changing interactions at low momentum transfer. Today, weak decays of hadrons containing heavy quarks are employed for tests of the Standard Model and measurements of its parameters. In particular, they offer the most direct way to determine the weak mixing angles, to test the unitarity of the Cabibbo–Kobayashi–Maskawa (CKM) matrix, and to explore the physics of CP violation. On the other hand, hadronic weak decays also serve as a probe of that part of strong-interaction phenomenology which is least understood: the confinement of quarks and gluons inside hadrons.

The structure of weak interactions in the Standard Model is rather simple. Flavour-changing decays are mediated by the coupling of the charged current J_{CC}^μ to the W -boson field:

$$\mathcal{L}_{CC} = -\frac{g}{\sqrt{2}} J_{CC}^\mu W_\mu^\dagger + \text{h.c.}, \quad (1)$$

where

$$J_{CC}^\mu = (\bar{\nu}_e, \bar{\nu}_\mu, \bar{\nu}_\tau) \gamma^\mu \begin{pmatrix} e_L \\ \mu_L \\ \tau_L \end{pmatrix} + (\bar{u}_L, \bar{c}_L, \bar{t}_L) \gamma^\mu V_{CKM} \begin{pmatrix} d_L \\ s_L \\ b_L \end{pmatrix} \quad (2)$$

contains the left-handed lepton and quark fields, and

$$V_{CKM} = \begin{pmatrix} V_{ud} & V_{us} & V_{ub} \\ V_{cd} & V_{cs} & V_{cb} \\ V_{td} & V_{ts} & V_{tb} \end{pmatrix} \quad (3)$$

is the CKM matrix. At low energies, the charged-current interaction gives rise to

2 Introduction

local four-fermion couplings of the form

$$\mathcal{L}_{\text{eff}} = -2\sqrt{2}G_F J_{CC}^\mu J_{CC,\mu}^\dagger, \quad (4)$$

where

$$G_F = \frac{g^2}{8M_W^2} = 1.16639(2) \text{ GeV}^{-2} \quad (5)$$

is the Fermi constant.

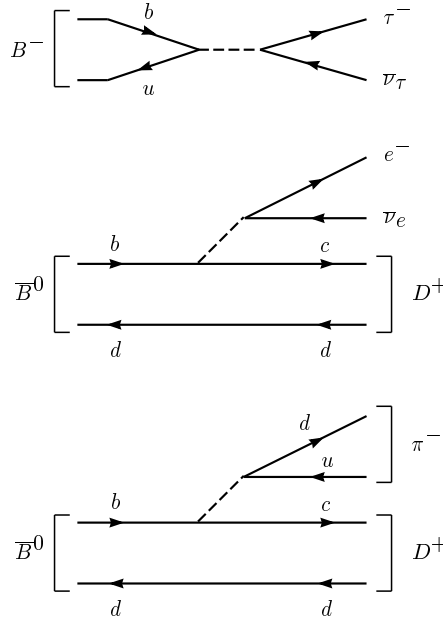


Figure 1: Examples of leptonic ($B^- \rightarrow \tau^- \bar{\nu}_\tau$), semileptonic ($\bar{B}^0 \rightarrow D^+ e^- \bar{\nu}_e$), and non-leptonic ($\bar{B}^0 \rightarrow D^+ \pi^-$) decays of B mesons.

According to the structure of the charged-current interaction, weak decays of hadrons can be divided into three classes: leptonic decays, in which the quarks of the decaying hadron annihilate each other and only leptons appear in the final state; semileptonic decays, in which both leptons and hadrons appear in the final state; and non-leptonic decays, in which the final state consists of hadrons only. Representative examples of these three types of decays are shown in Fig. 1. The simple quark-line graphs shown in this figure are a gross oversimplification, however. In the real world, quarks are confined inside hadrons, bound by the exchange of soft gluons. The simplicity of the weak interactions is overshadowed by the complexity of the strong interactions. A complicated interplay between the weak and strong forces characterizes the phenomenology of hadronic weak decays. As an example, a more realistic picture of a non-leptonic decay is shown in Fig. 2.

The complexity of strong-interaction effects increases with the number of quarks appearing in the final state. Bound-state effects in leptonic decays can be lumped

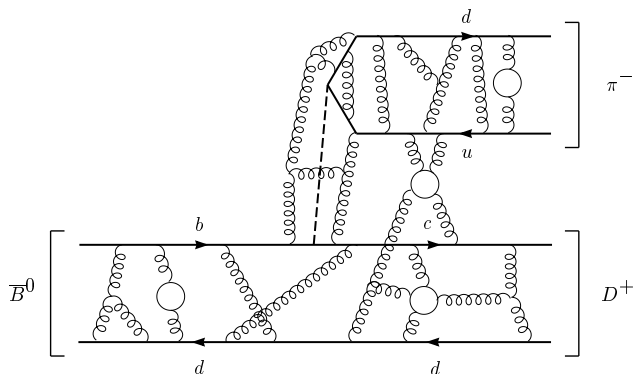


Figure 2: More realistic representation of a non-leptonic decay.

into a single parameter (a “decay constant”), while those in semileptonic decays are described by invariant form factors, depending on the momentum transfer q^2 between the hadrons. Approximate symmetries of the strong interactions help to constrain the properties of these form factors. For non-leptonic decays, on the other hand, we are still far from having a quantitative understanding of strong-interaction effects even in the simplest decay modes.

Over the last decade, a lot of information on heavy-quark decays has been collected in experiments at e^+e^- storage rings operating at the $\Upsilon(4s)$ resonance, and more recently at high-energy e^+e^- and hadron colliders. This has led to a rather detailed knowledge of the flavour sector of the Standard Model and many of the parameters associated with it. There have been several great discoveries in this field, such as $B^0-\bar{B}^0$ mixing^{1,2}, $b \rightarrow u$ transitions³⁻⁵, and rare decays induced by penguin operators^{6,7}. Yet there is much more to come. Upgrades of the existing facilities at Cornell and Fermilab, as well as the B -factories to be operated at SLAC, KEK, HERA-B and LHC-B, will provide a wealth of new results within the coming years. The experimental progress in heavy-flavour physics has been accompanied by a significant progress in theory, which was related to the discovery of heavy-quark symmetry, the development of the heavy-quark effective theory, and the establishment of the heavy-quark expansion for inclusive decay rates. The excitement about these developments is caused by the fact that they allow (some) model-independent predictions in an area in which “progress” in theory often meant nothing more than the construction of a new model, which could be used to estimate some strong-interaction hadronic matrix elements. In section , we explain the physical picture behind heavy-quark symmetry and discuss the construction, as well as simple applications, of the heavy-quark effective theory. Section 2 deals with applications of these concepts to exclusive weak decays of B mesons. Applications of the heavy-quark expansion to the description of inclusive decay rates and lifetimes of b hadrons are the topic of section 3. Section 5 is devoted to a discussion of CP violation in meson decays and the physics of the unitarity triangle.

2. Heavy-Quark Symmetry

This section provides an introduction to the ideas of heavy-quark symmetry^{8–13} and the heavy-quark effective theory^{14–24}, which provide the modern theoretical framework for the description of the properties and decays of hadrons containing a heavy quark. For a more detailed description of this subject, the reader is referred to the review articles in Refs.^{25–30}.

2.1. *The Physical Picture*

There are several reasons why the strong interactions of systems containing heavy quarks are easier to understand than those of systems containing only light quarks. The first is asymptotic freedom, the fact that the effective coupling constant of QCD becomes weak in processes with large momentum transfer, corresponding to interactions at short-distance scales^{31,32}. At large distances, on the other hand, the coupling becomes strong, leading to non-perturbative phenomena such as the confinement of quarks and gluons on a length scale $R_{\text{had}} \sim 1/\Lambda_{\text{QCD}} \sim 1$ fm, which determines the size of hadrons. Roughly speaking, $\Lambda_{\text{QCD}} \sim 0.2$ GeV is the energy scale that separates the regions of large and small coupling constant. When the mass of a quark Q is much larger than this scale, $m_Q \gg \Lambda_{\text{QCD}}$, it is called a heavy quark. The quarks of the Standard Model fall naturally into two classes: up, down and strange are light quarks, whereas charm, bottom and top are heavy quarks^a. For heavy quarks, the effective coupling constant $\alpha_s(m_Q)$ is small, implying that on length scales comparable to the Compton wavelength $\lambda_Q \sim 1/m_Q$ the strong interactions are perturbative and much like the electromagnetic interactions. In fact, the quarkonium systems ($\bar{Q}Q$), whose size is of order $\lambda_Q/\alpha_s(m_Q) \ll R_{\text{had}}$, are very much hydrogen-like. Since the discovery of asymptotic freedom, their properties could be predicted³³ before the observation of charmonium, and later of bottomonium states.

Systems composed of a heavy quark and other light constituents are more complicated. The size of such systems is determined by R_{had} , and the typical momenta exchanged between the heavy and light constituents are of order Λ_{QCD} . The heavy quark is surrounded by a most complicated, strongly interacting cloud of light quarks, antiquarks, and gluons. In this case it is the fact that $\lambda_Q \ll R_{\text{had}}$, i.e. that the Compton wavelength of the heavy quark is much smaller than the size of the hadron, which leads to simplifications. To resolve the quantum numbers of the heavy quark would require a hard probe; the soft gluons exchanged between the heavy quark and the light constituents can only resolve distances much larger than λ_Q . Therefore, the light degrees of freedom are blind to the flavour (mass) and spin orientation of the heavy quark. They experience only its colour field, which extends over large distances because of confinement. In the rest frame of the heavy quark, it is in fact only the electric colour field that is important; relativistic ef-

^aIronically, the top quark is of no relevance to my discussion here, since it is too heavy to form hadronic bound states before it decays.

fects such as colour magnetism vanish as $m_Q \rightarrow \infty$. Since the heavy-quark spin participates in interactions only through such relativistic effects, it decouples. That the heavy-quark mass becomes irrelevant can be seen as follows: as $m_Q \rightarrow \infty$, the heavy quark and the hadron that contains it have the same velocity. In the rest frame of the hadron, the heavy quark is at rest, too. The wave function of the light constituents follows from a solution of the field equations of QCD subject to the boundary condition of a static triplet source of colour at the location of the heavy quark. This boundary condition is independent of m_Q , and so is the solution for the configuration of the light constituents.

It follows that, in the limit $m_Q \rightarrow \infty$, hadronic systems which differ only in the flavour or spin quantum numbers of the heavy quark have the same configuration of their light degrees of freedom^{8–13}. Although this observation still does not allow us to calculate what this configuration is, it provides relations between the properties of such particles as the heavy mesons B , D , B^* and D^* , or the heavy baryons Λ_b and Λ_c (to the extent that corrections to the infinite quark-mass limit are small in these systems). These relations result from some approximate symmetries of the effective strong interactions of heavy quarks at low energies. The configuration of light degrees of freedom in a hadron containing a single heavy quark with velocity v does not change if this quark is replaced by another heavy quark with different flavour or spin, but with the same velocity. Both heavy quarks lead to the same static colour field. For N_h heavy-quark flavours, there is thus an $SU(2N_h)$ spin-flavour symmetry group, under which the effective strong interactions are invariant. These symmetries are in close correspondence to familiar properties of atoms. The flavour symmetry is analogous to the fact that different isotopes have the same chemistry, since to good approximation the wave function of the electrons is independent of the mass of the nucleus. The electrons only see the total nuclear charge. The spin symmetry is analogous to the fact that the hyperfine levels in atoms are nearly degenerate. The nuclear spin decouples in the limit $m_e/m_N \rightarrow 0$.

Heavy-quark symmetry is an approximate symmetry, and corrections arise since the quark masses are not infinite. In many respects, it is complementary to chiral symmetry, which arises in the opposite limit of small quark masses. There is an important distinction, however. Whereas chiral symmetry is a symmetry of the QCD Lagrangian in the limit of vanishing quark masses, heavy-quark symmetry is not a symmetry of the Lagrangian (not even an approximate one), but rather a symmetry of an effective theory, which is a good approximation of QCD in a certain kinematic region. It is realized only in systems in which a heavy quark interacts predominantly by the exchange of soft gluons. In such systems the heavy quark is almost on-shell; its momentum fluctuates around the mass shell by an amount of order Λ_{QCD} . The corresponding fluctuations in the velocity of the heavy quark vanish as $\Lambda_{\text{QCD}}/m_Q \rightarrow 0$. The velocity becomes a conserved quantity and is no longer a dynamical degree of freedom²¹. Nevertheless, results derived on the basis of heavy-quark symmetry are model-independent consequences of QCD in a well-defined limit. The symmetry-breaking corrections can, at least in principle, be

studied in a systematic way. To this end, it is however necessary to recast the QCD Lagrangian for a heavy quark,

$$\mathcal{L}_Q = \bar{Q} (i \not{D} - m_Q) Q, \quad (6)$$

into a form suitable for taking the limit $m_Q \rightarrow \infty$.

2.2. *Heavy-Quark Effective Theory*

The effects of a very heavy particle often become irrelevant at low energies. It is then useful to construct a low-energy effective theory, in which this heavy particle no longer appears. Eventually, this effective theory will be easier to deal with than the full theory. A familiar example is Fermi's theory of the weak interactions. For the description of weak decays of hadrons, the weak interactions can be approximated by point-like four-fermion couplings, governed by a dimensionful coupling constant G_F . Only at energies much larger than the masses of hadrons can the effects of the intermediate vector bosons, W and Z , be resolved.

The process of removing the degrees of freedom of a heavy particle involves the following steps^{34–36}: one first identifies the heavy-particle fields and “integrates them out” in the generating functional of the Green functions of the theory. This is possible since at low energies the heavy particle does not appear as an external state. However, although the action of the full theory is usually a local one, what results after this first step is a non-local effective action. The non-locality is related to the fact that in the full theory the heavy particle with mass M can appear in virtual processes and propagate over a short but finite distance $\Delta x \sim 1/M$. Thus, a second step is required to obtain a local effective Lagrangian: the non-local effective action is rewritten as an infinite series of local terms in an Operator Product Expansion (OPE)^{37,38}. Roughly speaking, this corresponds to an expansion in powers of $1/M$. It is in this step that the short- and long-distance physics is disentangled. The long-distance physics corresponds to interactions at low energies and is the same in the full and the effective theory. But short-distance effects arising from quantum corrections involving large virtual momenta (of order M) are not reproduced in the effective theory, once the heavy particle has been integrated out. In a third step, they have to be added in a perturbative way using renormalization-group techniques. These short-distance effects lead to a renormalization of the coefficients of the local operators in the effective Lagrangian. An example is the effective Lagrangian for non-leptonic weak decays, in which radiative corrections from hard gluons with virtual momenta in the range between m_W and some renormalization scale $\mu \sim 1$ GeV give rise to Wilson coefficients, which renormalize the local four-fermion interactions^{39–41}.

The heavy-quark effective theory (HQET) is constructed to provide a simplified description of processes where a heavy quark interacts with light degrees of freedom by the exchange of soft gluons^{14–24}. Clearly, m_Q is the high-energy scale in this case, and Λ_{QCD} is the scale of the hadronic physics we are interested in. However, a subtlety arises since we want to describe the properties and decays of hadrons

which contain a heavy quark. Hence, it is not possible to remove the heavy quark completely from the effective theory. What is possible, however, is to integrate out the “small components” in the full heavy-quark spinor, which describe the fluctuations around the mass shell.

The starting point in the construction of the low-energy effective theory is the observation that a very heavy quark bound inside a hadron moves more or less with the hadron’s velocity v , and is almost on-shell. Its momentum can be written as

$$p_Q^\mu = m_Q v^\mu + k^\mu, \quad (7)$$

where the components of the so-called residual momentum k are much smaller than m_Q . Note that v is a four-velocity, so that $v^2 = 1$. Interactions of the heavy quark with light degrees of freedom change the residual momentum by an amount of order $\Delta k \sim \Lambda_{\text{QCD}}$, but the corresponding changes in the heavy-quark velocity vanish as $\Lambda_{\text{QCD}}/m_Q \rightarrow 0$. In this situation, it is appropriate to introduce large- and small-component fields h_v and H_v by

$$h_v(x) = e^{im_Q v \cdot x} P_+ Q(x), \quad H_v(x) = e^{im_Q v \cdot x} P_- Q(x), \quad (8)$$

where P_+ and P_- are projection operators defined as

$$P_\pm = \frac{1 \pm \not{v}}{2}. \quad (9)$$

It follows that

$$Q(x) = e^{-im_Q v \cdot x} [h_v(x) + H_v(x)]. \quad (10)$$

Because of the projection operators, the new fields satisfy $\not{v} h_v = h_v$ and $\not{v} H_v = -H_v$. In the rest frame, i.e. for $v^\mu = (1, 0, 0, 0)$, h_v corresponds to the upper two components of Q , while H_v corresponds to the lower ones. Whereas h_v annihilates a heavy quark with velocity v , H_v creates a heavy antiquark with velocity v .

In terms of the new fields, the QCD Lagrangian (6) for a heavy quark takes the form

$$\mathcal{L}_Q = \bar{h}_v i v \cdot D h_v - \bar{H}_v (i v \cdot D + 2m_Q) H_v + \bar{h}_v i \not{D}_\perp H_v + \bar{H}_v i \not{D}_\perp h_v, \quad (11)$$

where $D_\perp^\mu = D^\mu - v^\mu v \cdot D$ is orthogonal to the heavy-quark velocity: $v \cdot D_\perp = 0$. In the rest frame, $D_\perp^\mu = (0, \vec{D})$ contains the spatial components of the covariant derivative. From (11), it is apparent that h_v describes massless degrees of freedom, whereas H_v corresponds to fluctuations with twice the heavy-quark mass. These are the heavy degrees of freedom that will be eliminated in the construction of the effective theory. The fields are mixed by the presence of the third and fourth terms, which describe pair creation or annihilation of heavy quarks and antiquarks. As shown in the first diagram in Fig. 3, in a virtual process, a heavy quark propagating forward in time can turn into an antiquark propagating backward in time, and then turn back into a quark. The energy of the intermediate quantum state $hh\bar{H}$ is larger than the energy of the incoming heavy quark by at least $2m_Q$. Because of

this large energy gap, the virtual quantum fluctuation can only propagate over a short distance $\Delta x \sim 1/m_Q$. On hadronic scales set by $R_{\text{had}} = 1/\Lambda_{\text{QCD}}$, the process essentially looks like a local interaction of the form

$$\bar{h}_v i \not{D}_\perp \frac{1}{2m_Q} i \not{D}_\perp h_v, \quad (12)$$

where we have simply replaced the propagator for H_v by $1/2m_Q$. A more correct treatment is to integrate out the small-component field H_v , thereby deriving a non-local effective action for the large-component field h_v , which can then be expanded in terms of local operators. Before doing this, let us mention a second type of virtual corrections involving pair creation, namely heavy-quark loops. An example is shown in the second diagram in Fig. 3. Heavy-quark loops cannot be described in terms of the effective fields h_v and H_v , since the quark velocities inside a loop are not conserved and are in no way related to hadron velocities. However, such short-distance processes are proportional to the small coupling constant $\alpha_s(m_Q)$ and can be calculated in perturbation theory. They lead to corrections that are added onto the low-energy effective theory in the renormalization procedure.

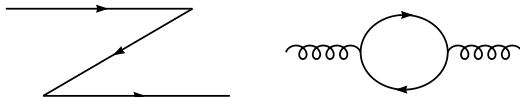


Figure 3: Virtual fluctuations involving pair creation of heavy quarks. Time flows to the right.

On a classical level, the heavy degrees of freedom represented by H_v can be eliminated using the equation of motion $(i \not{D} - m_Q) Q = 0$. With (10), this gives

$$i \not{D} h_v + (i \not{D} - 2m_Q) H_v = 0, \quad (13)$$

and multiplying by P_\pm one derives the two equations

$$-iv \cdot D h_v = i \not{D}_\perp H_v, \quad (iv \cdot D + 2m_Q) H_v = i \not{D}_\perp h_v. \quad (14)$$

The second one can be solved to give

$$H_v = \frac{1}{2m_Q + iv \cdot D} i \not{D}_\perp h_v, \quad (15)$$

which shows that the small-component field H_v is indeed of order $1/m_Q$. We can now insert this solution into the first equation to obtain the equation of motion for h_v . It is easy to see that this equation follows from the non-local effective Lagrangian

$$\mathcal{L}_{\text{eff}} = \bar{h}_v iv \cdot D h_v + \bar{h}_v i \not{D}_\perp \frac{1}{2m_Q + iv \cdot D} i \not{D}_\perp h_v. \quad (16)$$

Clearly, the second term corresponds to the first class of virtual processes shown in Fig. 3.

Another symmetry of the HQET arises since the mass of the heavy quark does not appear in the effective Lagrangian. For N_h heavy quarks moving at the same velocity, eq. (20) can be extended by writing

$$\mathcal{L}_\infty = \sum_{i=1}^{N_h} \bar{h}_v^i i v \cdot D h_v^i. \quad (23)$$

This is invariant under rotations in flavour space. When combined with the spin symmetry, the symmetry group is promoted to $SU(2N_h)$. This is the heavy-quark spin-flavour symmetry^{13,21}. Its physical content is that, in the limit $m_Q \rightarrow \infty$, the strong interactions of a heavy quark become independent of its mass and spin.

Consider now the operators appearing at order $1/m_Q$ in the effective Lagrangian (19). They are easiest to identify in the rest frame. The first operator,

$$\mathcal{O}_{\text{kin}} = \frac{1}{2m_Q} \bar{h}_v (iD_\perp)^2 h_v \rightarrow -\frac{1}{2m_Q} \bar{h}_v (i\vec{D})^2 h_v, \quad (24)$$

is the gauge-covariant extension of the kinetic energy arising from the off-shell residual motion of the heavy quark. The second operator is the non-Abelian analogue of the Pauli interaction, which describes the colour-magnetic coupling of the heavy-quark spin to the gluon field:

$$\mathcal{O}_{\text{mag}} = \frac{g_s}{4m_Q} \bar{h}_v \sigma_{\mu\nu} G^{\mu\nu} h_v \rightarrow -\frac{g_s}{m_Q} \bar{h}_v \vec{S} \cdot \vec{B}_c h_v. \quad (25)$$

Here \vec{S} is the spin operator defined in (21), and $B_c^i = -\frac{1}{2}\epsilon^{ijk}G^{jk}$ are the components of the colour-magnetic field. The chromo-magnetic interaction is a relativistic effect, which scales like $1/m_Q$. This is the origin of the heavy-quark spin symmetry.

2.3. Spectroscopic Implications

The spin-flavour symmetry leads to many interesting relations between the properties of hadrons containing a heavy quark. The most direct consequences concern the spectroscopy of such states⁴². In the limit $m_Q \rightarrow \infty$, the spin of the heavy quark and the total angular momentum j of the light degrees of freedom are separately conserved by the strong interactions. Because of heavy-quark symmetry, the dynamics is independent of the spin and mass of the heavy quark. Hadronic states can thus be classified by the quantum numbers (flavour, spin, parity, etc.) of the light degrees of freedom⁴³. The spin symmetry predicts that, for fixed $j \neq 0$, there is a doublet of degenerate states with total spin $J = j \pm \frac{1}{2}$. The flavour symmetry relates the properties of states with different heavy-quark flavour.

In general, the mass of a hadron H_Q containing a heavy quark Q obeys an expansion of the form

$$m_H = m_Q + \bar{\Lambda} + \frac{\Delta m^2}{2m_Q} + O(1/m_Q^2). \quad (26)$$

The parameter $\bar{\Lambda}$ represents contributions arising from terms in the Lagrangian that are independent of the heavy-quark mass⁴⁴, whereas the quantity Δm^2 originates from the terms of order $1/m_Q$ in the effective Lagrangian of the HQET. For the ground-state pseudoscalar and vector mesons, one can parametrize the contributions from the kinetic energy and the chromo-magnetic interaction in terms of two quantities λ_1 and λ_2 , in such a way that⁴⁵

$$\Delta m^2 = -\lambda_1 + 2 \left[J(J+1) - \frac{3}{2} \right] \lambda_2. \quad (27)$$

The hadronic parameters $\bar{\Lambda}$, λ_1 and λ_2 are independent of m_Q . They characterize the properties of the light constituents.

Consider, as a first example, the SU(3) mass splittings for heavy mesons. The heavy-quark expansion predicts that

$$\begin{aligned} m_{B_S} - m_{B_d} &= \bar{\Lambda}_s - \bar{\Lambda}_d + O(1/m_b), \\ m_{D_S} - m_{D_d} &= \bar{\Lambda}_s - \bar{\Lambda}_d + O(1/m_c), \end{aligned} \quad (28)$$

where we have indicated that the value of the parameter $\bar{\Lambda}$ depends on the flavour of the light quark. Thus, to the extent that the charm and bottom quarks can both be considered sufficiently heavy, the mass splittings should be similar in the two systems. This prediction is confirmed experimentally, since⁴⁶

$$\begin{aligned} m_{B_S} - m_{B_d} &= (90 \pm 3) \text{ MeV}, \\ m_{D_S} - m_{D_d} &= (99 \pm 1) \text{ MeV}. \end{aligned} \quad (29)$$

As a second example, consider the spin splittings between the ground-state pseudoscalar ($J = 0$) and vector ($J = 1$) mesons, which are the members of the spin-doublet with $j = \frac{1}{2}$. The theory predicts that

$$\begin{aligned} m_{B^*}^2 - m_B^2 &= 4\lambda_2 + O(1/m_b), \\ m_{D^*}^2 - m_D^2 &= 4\lambda_2 + O(1/m_c). \end{aligned} \quad (30)$$

The data are compatible with this:

$$\begin{aligned} m_{B^*}^2 - m_B^2 &\simeq 0.49 \text{ GeV}^2, \\ m_{D^*}^2 - m_D^2 &\simeq 0.55 \text{ GeV}^2. \end{aligned} \quad (31)$$

Assuming that the B system is close to the heavy-quark limit, we obtain the value

$$\lambda_2 \simeq 0.12 \text{ GeV}^2 \quad (32)$$

for one of the hadronic parameters in (27). This quantity plays an important role in the phenomenology of inclusive decays of heavy hadrons.

A third example is provided by the mass splittings between the ground-state mesons and baryons containing a heavy quark. The HQET predicts that

$$\begin{aligned} m_{\Lambda_b} - m_B &= \bar{\Lambda}_{\text{baryon}} - \bar{\Lambda}_{\text{meson}} + O(1/m_b), \\ m_{\Lambda_c} - m_D &= \bar{\Lambda}_{\text{baryon}} - \bar{\Lambda}_{\text{meson}} + O(1/m_c). \end{aligned} \quad (33)$$

This is again consistent with the experimental results

$$\begin{aligned} m_{\Lambda_b} - m_B &= (346 \pm 6) \text{ MeV}, \\ m_{\Lambda_c} - m_D &= (416 \pm 1) \text{ MeV}, \end{aligned} \quad (34)$$

although in this case the data indicate sizeable symmetry-breaking corrections. For the mass of the Λ_b baryon, we have used the value

$$m_{\Lambda_b} = (5625 \pm 6) \text{ MeV}, \quad (35)$$

which is obtained by averaging the result $m_{\Lambda_b} = (5639 \pm 15) \text{ MeV}$ quoted in Ref.⁴⁶ with the preliminary value $m_{\Lambda_b} = (5623 \pm 5 \pm 4) \text{ MeV}$ reported by the CDF Collaboration⁴⁷. The dominant correction to the relations (33) comes from the contribution of the chromo-magnetic interaction to the masses of the heavy mesons^b, which adds a term $3\lambda_2/2m_Q$ on the right-hand side. Including this term, we obtain the refined prediction that the two quantities

$$\begin{aligned} m_{\Lambda_b} - m_B - \frac{3\lambda_2}{2m_B} &= (312 \pm 6) \text{ MeV}, \\ m_{\Lambda_c} - m_D - \frac{3\lambda_2}{2m_D} &= (320 \pm 1) \text{ MeV} \end{aligned} \quad (36)$$

should be close to each other. This is clearly satisfied by the data.

The mass formula (26) can also be used to derive information on the heavy-quark masses from the observed hadron masses. Introducing the “spin-averaged” meson masses $\bar{m}_B = \frac{1}{4}(m_B + 3m_{B^*}) \simeq 5.31 \text{ GeV}$ and $\bar{m}_D = \frac{1}{4}(m_D + 3m_{D^*}) \simeq 1.97 \text{ GeV}$, we find that

$$m_b - m_c = (\bar{m}_B - \bar{m}_D) \left\{ 1 - \frac{\lambda_1}{2\bar{m}_B\bar{m}_D} + O(1/m_Q^3) \right\}. \quad (37)$$

Using theoretical estimates for the parameter λ_1 , which lie in the range^{48–50}

$$\lambda_1 = -(0.4 \pm 0.2) \text{ GeV}^2, \quad (38)$$

this relation leads to

$$m_b - m_c = (3.40 \pm 0.03 \pm 0.03) \text{ GeV}, \quad (39)$$

where the first error reflects the uncertainty in the value of λ_1 , and the second one takes into account unknown higher-order corrections. As will be discussed in section 3, the fact that the difference $(m_b - m_c)$ is determined rather precisely becomes important in the analysis of inclusive decays of heavy hadrons.

For completeness, we note that for the pole masses of the heavy quarks we shall adopt the values

$$m_b = 4.8 \text{ GeV}, \quad m_c = 1.4 \text{ GeV}. \quad (40)$$

^bBecause of the spin symmetry, there is no such contribution to the masses of the Λ_Q baryons.

The concept of the pole mass of a heavy quark has been the subject of much discussion recently. It has been found that there is an unavoidable ambiguity of order Λ_{QCD} in any definition of the pole mass extending beyond perturbation theory^{51,52}. Formally, this ambiguity appears as a divergence of the perturbation series, which relates the pole mass to a renormalized mass defined at short distances, such as the “running mass” $\overline{m}_Q(m_Q)$. As long as we work to a finite order in perturbation theory, however, this subtlety can be ignored. The values given above will be used in connection with one-loop calculations and thus refer to the one-loop pole masses of the heavy quarks.

3. Exclusive Semileptonic Decays

Semileptonic decays of B mesons have received a lot of attention in recent years. The decay channel $\bar{B} \rightarrow D^* \ell \bar{\nu}$ has the largest branching fraction of all B -meson decay modes. From a theoretical point of view, semileptonic decays are simple enough to allow for a reliable, quantitative description. The analysis of these decays provides much information about the strong forces that bind the quarks and gluons into hadrons. Schematically, a semileptonic decay process is shown in Fig. 5. The strength of the $b \rightarrow c$ transition vertex is governed by the element V_{cb} of the CKM matrix. The parameters of this matrix are fundamental parameters of the Standard Model. A primary goal of the study of semileptonic decays of B mesons is to extract with high precision the values of $|V_{cb}|$ and $|V_{ub}|$. In this lecture, we will discuss the theoretical basis of such analyses.

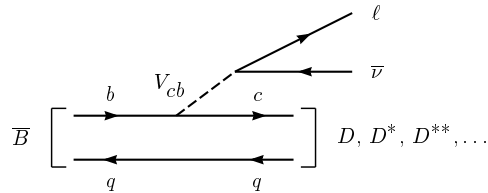


Figure 5: Semileptonic decays of a B meson.

3.1. Weak Decay Form Factors

Heavy-quark symmetry implies relations between the weak decay form factors of heavy mesons, which are of particular interest. These relations have been derived by Isgur and Wise¹³, generalizing ideas developed by Nussinov and Wetzel¹⁰, and by Voloshin and Shifman^{11,12}.

Consider the elastic scattering of a B meson, $\bar{B}(v) \rightarrow \bar{B}(v')$, induced by a vector current coupled to the b quark. Before the action of the current, the light degrees of freedom in the B meson orbit around the heavy quark, which acts as a static source of colour. On average, the b quark and the B meson have the same velocity v . The action of the current is to replace instantaneously (at $t = t_0$) the colour source by one moving at a velocity v' , as indicated in Fig. 6. If $v = v'$, nothing

happens; the light degrees of freedom do not realize that there was a current acting on the heavy quark. If the velocities are different, however, the light constituents suddenly find themselves interacting with a moving colour source. Soft gluons have to be exchanged to rearrange them so as to form a B meson moving at velocity v' . This rearrangement leads to a form-factor suppression, which reflects the fact that as the velocities become more and more different, the probability for an elastic transition decreases. The important observation is that, in the limit $m_b \rightarrow \infty$, the form factor can only depend on the Lorentz boost $\gamma = v \cdot v'$ that connects the rest frames of the initial- and final-state mesons. Thus, in this limit a dimensionless probability function $\xi(v \cdot v')$ describes the transition. It is called the Isgur–Wise function¹³. In the HQET, which provides the appropriate framework for taking the limit $m_b \rightarrow \infty$, the hadronic matrix element describing the scattering process can thus be written as

$$\frac{1}{m_B} \langle \bar{B}(v') | \bar{b}_{v'} \gamma^\mu b_v | \bar{B}(v) \rangle = \xi(v \cdot v') (v + v')^\mu. \quad (41)$$

Here, b_v and $b_{v'}$ are the velocity-dependent heavy-quark fields defined in (8). It is important that the function $\xi(v \cdot v')$ does not depend on m_b . The factor $1/m_B$ on the left-hand side compensates for a trivial dependence on the heavy-meson mass caused by the relativistic normalization of meson states, which is conventionally taken to be

$$\langle \bar{B}(p') | \bar{B}(p) \rangle = 2m_B v^0 (2\pi)^3 \delta^3(\vec{p} - \vec{p}'). \quad (42)$$

Note that there is no term proportional to $(v - v')^\mu$ in (41). This can be seen by contracting the matrix element with $(v - v')_\mu$, which must give zero since $\not{v} b_v = b_v$ and $\bar{b}_{v'} \not{v}' = \bar{b}_{v'}$.

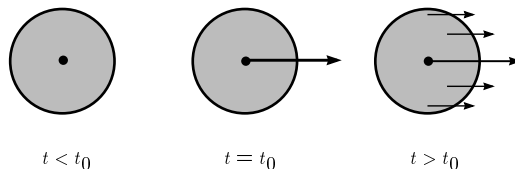


Figure 6: Elastic transition induced by an external heavy-quark current.

It is more conventional to write the above matrix element in terms of an elastic form factor $F_{\text{el}}(q^2)$ depending on the momentum transfer $q^2 = (p - p')^2$:

$$\langle \bar{B}(v') | \bar{b} \gamma^\mu b | \bar{B}(v) \rangle = F_{\text{el}}(q^2) (p + p')^\mu, \quad (43)$$

where $p^{(\prime)} = m_B v^{(\prime)}$. Comparing this with (41), we find that

$$F_{\text{el}}(q^2) = \xi(v \cdot v'), \quad q^2 = -2m_B^2(v \cdot v' - 1). \quad (44)$$

Because of current conservation, the elastic form factor is normalized to unity at $q^2 = 0$. This condition implies the normalization of the Isgur–Wise function at the

kinematic point $v \cdot v' = 1$, i.e. for $v = v'$:

$$\xi(1) = 1. \quad (45)$$

It is in accordance with the intuitive argument that the probability for an elastic transition is unity if there is no velocity change. Since for $v = v'$ the daughter meson is at rest in the rest frame of the parent meson, the point $v \cdot v' = 1$ is referred to as the zero-recoil limit.

We can now use the flavour symmetry to replace the b quark in the final-state meson by a c quark, thereby turning the B meson into a D meson. Then the scattering process turns into a weak decay process. In the infinite mass limit, the replacement $b_{v'} \rightarrow c_{v'}$ is a symmetry transformation, under which the effective Lagrangian is invariant. Hence, the matrix element

$$\frac{1}{\sqrt{m_B m_D}} \langle D(v') | \bar{c}_{v'} \gamma^\mu b_v | \bar{B}(v) \rangle = \xi(v \cdot v') (v + v')^\mu \quad (46)$$

is still determined by the same function $\xi(v \cdot v')$. This is interesting, since in general the matrix element of a flavour-changing current between two pseudoscalar mesons is described by two form factors:

$$\langle D(v') | \bar{c} \gamma^\mu b | \bar{B}(v) \rangle = f_+(q^2) (p + p')^\mu - f_-(q^2) (p - p')^\mu. \quad (47)$$

Comparing the above two equations, we find that

$$\begin{aligned} f_\pm(q^2) &= \frac{m_B \pm m_D}{2\sqrt{m_B m_D}} \xi(v \cdot v'), \\ q^2 &= m_B^2 + m_D^2 - 2m_B m_D (v \cdot v' - 1). \end{aligned} \quad (48)$$

Thus, the heavy-quark flavour symmetry relates two *a priori* independent form factors to one and the same function. Moreover, the normalization of the Isgur–Wise function at $v \cdot v' = 1$ now implies a non-trivial normalization of the form factors $f_\pm(q^2)$ at the point of maximum momentum transfer, $q_{\max}^2 = (m_B - m_D)^2$:

$$f_\pm(q_{\max}^2) = \frac{m_B \pm m_D}{2\sqrt{m_B m_D}}. \quad (49)$$

The heavy-quark spin symmetry leads to additional relations among weak decay form factors. It can be used to relate matrix elements involving vector mesons to those involving pseudoscalar mesons. A vector meson with longitudinal polarization is related to a pseudoscalar meson by a rotation of the heavy-quark spin. Hence, the spin-symmetry transformation $c_{v'}^\uparrow \rightarrow c_{v'}^\downarrow$ relates the transition matrix element for $\bar{B} \rightarrow D$ to that for $\bar{B} \rightarrow D^*$. The result of this transformation is¹³:

$$\begin{aligned} \frac{1}{\sqrt{m_B m_{D^*}}} \langle D^*(v', \epsilon) | \bar{c}_{v'} \gamma^\mu b_v | \bar{B}(v) \rangle &= i \epsilon^{\mu\nu\alpha\beta} \epsilon_\nu^* v'_\alpha v_\beta \xi(v \cdot v'), \\ \frac{1}{\sqrt{m_B m_{D^*}}} \langle D^*(v', \epsilon) | \bar{c}_{v'} \gamma^\mu \gamma_5 b_v | \bar{B}(v) \rangle &= \left[\epsilon^{*\mu} (v \cdot v' + 1) - v'^\mu \epsilon^* \cdot v \right] \xi(v \cdot v'), \end{aligned} \quad (50)$$

where ϵ denotes the polarization vector of the D^* meson. Once again, the matrix elements are completely described in terms of the Isgur–Wise function. Now this is even more remarkable, since in general four form factors, $V(q^2)$ for the vector current, and $A_i(q^2)$, $i = 0, 1, 2$, for the axial vector current, are required to parametrize these matrix elements. In the heavy-quark limit, they obey the relations⁵³

$$\begin{aligned} \xi(v \cdot v') &= V(q^2) = A_0(q^2) = A_1(q^2) = \left[1 - \frac{q^2}{(m_B + m_D)^2}\right]^{-1} A_1(q^2), \\ q^2 &= m_B^2 + m_{D^*}^2 - 2m_B m_{D^*} (v \cdot v' - 1). \end{aligned} \quad (51)$$

Equations (48) and (51) summarize the relations imposed by heavy-quark symmetry on the weak decay form factors describing the semileptonic decay processes $\bar{B} \rightarrow D \ell \bar{\nu}$ and $\bar{B} \rightarrow D^* \ell \bar{\nu}$. These relations are model-independent consequences of QCD in the limit where $m_b, m_c \gg \Lambda_{\text{QCD}}$. They play a crucial role in the determination of $|V_{cb}|$. In terms of the recoil variable $w = v \cdot v'$, the differential semileptonic decay rates in the heavy-quark limit become:

$$\begin{aligned} \frac{d\Gamma(\bar{B} \rightarrow D \ell \bar{\nu})}{dw} &= \frac{G_F^2}{48\pi^3} |V_{cb}|^2 (m_B + m_D)^2 m_D^3 (w^2 - 1)^{3/2} \xi^2(w), \\ \frac{d\Gamma(\bar{B} \rightarrow D^* \ell \bar{\nu})}{dw} &= \frac{G_F^2}{48\pi^3} |V_{cb}|^2 (m_B - m_{D^*})^2 m_{D^*}^3 \sqrt{w^2 - 1} (w + 1)^2 \\ &\quad \times \left[1 + \frac{4w}{w + 1} \frac{m_B^2 - 2w m_B m_{D^*} + m_{D^*}^2}{(m_B - m_{D^*})^2}\right] \xi^2(w). \end{aligned} \quad (52)$$

These expressions receive symmetry-breaking corrections, since the masses of the heavy quarks are not infinitely large. Perturbative corrections of order $\alpha_s^n(m_Q)$, with $Q = b$ or c , can be calculated order by order in perturbation theory. A more difficult task is to control non-perturbative power corrections of order $(\Lambda_{\text{QCD}}/m_Q)^n$. The HQET provides a systematic framework for analysing these corrections. As an example, we have discussed in section the $1/m_Q$ corrections to the effective Lagrangian. For the more complicated case of weak-decay form factors, the analysis of the $1/m_Q$ corrections was performed by Luke⁵⁴. Later, Falk and the present author have also analysed the structure of $1/m_Q^2$ corrections for both meson and baryon weak decay form factors⁴⁵. We shall not discuss these rather technical issues in detail, but only mention the most important result of Luke’s analysis. It concerns the zero-recoil limit, where an analogue of the Ademollo–Gatto theorem⁵⁵ can be proved. This is Luke’s theorem⁵⁴, which states that the matrix elements describing the leading $1/m_Q$ corrections to weak decay amplitudes vanish at zero recoil. This theorem is valid to all orders in perturbation theory^{45,56,57}. Most importantly, it protects the $\bar{B} \rightarrow D^* \ell \bar{\nu}$ decay rate from receiving first-order $1/m_Q$ corrections at zero recoil⁵⁸. A similar statement is not true for the decay $\bar{B} \rightarrow D \ell \bar{\nu}$, however. The reason is simple but somewhat subtle. Luke’s theorem protects only those form factors not multiplied by kinematic factors that vanish for $v = v'$. By angular momentum conservation, the two pseudoscalar mesons in the decay $\bar{B} \rightarrow D \ell \bar{\nu}$ must

be in a relative p -wave, and hence the amplitude is proportional to the velocity $|\vec{v}_D|$ of the D meson in the B -meson rest frame. This leads to a factor $(w^2 - 1)$ in the decay rate. In such a situation, form factors that are kinematically suppressed can contribute⁵³.

3.2. Short-Distance Corrections

In section , we have discussed the first two steps in the construction of the HQET. Integrating out the small components in the heavy-quark fields, a non-local effective action was derived, which was then expanded in a series of local operators. The effective Lagrangian derived that way correctly reproduces the long-distance physics of the full theory. It does not contain the short-distance physics correctly, however. The reason is obvious: a heavy quark participates in strong interactions through its coupling to gluons. These gluons can be soft or hard, i.e. their virtual momenta can be small, of the order of the confinement scale, or large, of the order of the heavy-quark mass. But hard gluons can resolve the spin and flavour quantum numbers of a heavy quark. Their effects lead to a renormalization of the coefficients of the operators in the HQET. A new feature of such short-distance corrections is that through the running coupling constant $\alpha_s(m_Q)$ they induce a logarithmic dependence on the heavy-quark mass¹¹. Fortunately, since $\alpha_s(m_Q)$ is small, these effects can be calculated in perturbation theory.

Consider, as an example, matrix elements of the vector current $V = \bar{q}\gamma^\mu Q$. In QCD this current is partially conserved and needs no renormalization⁵⁹. Its matrix elements are free of ultraviolet divergences. Still, these matrix elements have a logarithmic dependence on m_Q from the exchange of hard gluons with virtual momenta of the order of the heavy-quark mass. If one goes over to the effective theory by taking the limit $m_Q \rightarrow \infty$, these logarithms diverge. Consequently, the vector current in the effective theory does require a renormalization¹⁸. Its matrix elements depend on an arbitrary renormalization scale μ , which separates the regions of short- and long-distance physics. If μ is chosen such that $\Lambda_{\text{QCD}} \ll \mu \ll m_Q$, the effective coupling constant in the region between μ and m_Q is small, and perturbation theory can be used to compute the short-distance corrections. These corrections have to be added to the matrix elements of the effective theory, which contain the long-distance physics below the scale μ . Schematically, then, the relation between matrix elements in the full and in the effective theory is

$$\langle V(m_Q) \rangle_{\text{QCD}} = C_0(m_Q, \mu) \langle V_0(\mu) \rangle_{\text{HQET}} + \frac{C_1(m_Q, \mu)}{m_Q} \langle V_1(\mu) \rangle_{\text{HQET}} + \dots, \quad (53)$$

where we have indicated that matrix elements in the full theory depend on m_Q , whereas matrix elements in the effective theory are mass-independent, but do depend on the renormalization scale. The Wilson coefficients $C_i(m_Q, \mu)$ are defined by this relation. Order by order in perturbation theory, they can be computed from a comparison of the matrix elements in the two theories. Since the effective theory is constructed to reproduce correctly the low-energy behaviour of the full theory, this

“matching” procedure is independent of any long-distance physics, such as infrared singularities, non-perturbative effects, the nature of the external states used in the matrix elements, etc.

The calculation of the coefficient functions in perturbation theory uses the powerful methods of the renormalization group. It is in principle straightforward, yet in practice rather tedious. A comprehensive discussion of most of the existing calculations of short-distance corrections in the HQET can be found in Ref.²⁵.

3.3. Model-Independent Determination of $|V_{cb}|$

We will now discuss some of the most important applications and tests of the above formalism in the context of semileptonic decays of B mesons. A model-independent determination of the CKM matrix element $|V_{cb}|$ based on heavy-quark symmetry can be obtained by measuring the recoil spectrum of D^* mesons produced in $\bar{B} \rightarrow D^* \ell \bar{\nu}$ decays⁵⁸. In the heavy-quark limit, the differential decay rate for this process has been given in (52). In order to allow for corrections to that limit, we write

$$\begin{aligned} \frac{d\Gamma(\bar{B} \rightarrow D^* \ell \bar{\nu})}{dw} &= \frac{G_F^2}{48\pi^3} (m_B - m_{D^*})^2 m_{D^*}^3 \sqrt{w^2 - 1} (w + 1)^2 \\ &\times \left[1 + \frac{4w}{w + 1} \frac{m_B^2 - 2w m_B m_{D^*} + m_{D^*}^2}{(m_B - m_{D^*})^2} \right] |V_{cb}|^2 \mathcal{F}^2(w), \end{aligned} \quad (54)$$

where the hadronic form factor $\mathcal{F}(w)$ coincides with the Isgur–Wise function up to symmetry-breaking corrections of order $\alpha_s(m_Q)$ and Λ_{QCD}/m_Q . The idea is to measure the product $|V_{cb}| \mathcal{F}(w)$ as a function of w , and to extract $|V_{cb}|$ from an extrapolation of the data to the zero-recoil point $w = 1$, where the B and the D^* mesons have a common rest frame. At this kinematic point, heavy-quark symmetry helps to calculate the normalization $\mathcal{F}(1)$ with small and controlled theoretical errors. Since the range of w values accessible in this decay is rather small ($1 < w < 1.5$), the extrapolation can be done using an expansion around $w = 1$:

$$\mathcal{F}(w) = \mathcal{F}(1) \left[1 - \hat{\varrho}^2 (w - 1) + \dots \right]. \quad (55)$$

The slope $\hat{\varrho}^2$ is treated as a fit parameter.

Measurements of the recoil spectrum have been performed first by the ARGUS⁶⁰ and CLEO⁶¹ Collaborations in experiments operating at the $\Upsilon(4s)$ resonance, and more recently by the ALEPH⁶² and DELPHI⁶³ Collaborations at LEP. As an example, Fig. 7 shows the data reported by the CLEO Collaboration. The results obtained by the various experimental groups from a linear fit to their data are summarized in Table 1. The weighted average of these results is

$$\begin{aligned} |V_{cb}| \mathcal{F}(1) &= (34.6 \pm 1.7) \times 10^{-3}, \\ \hat{\varrho}^2 &= 0.82 \pm 0.09. \end{aligned} \quad (56)$$

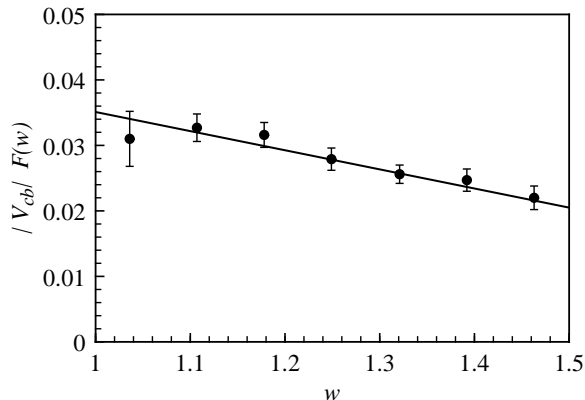


Figure 7: CLEO data for the product $|V_{cb}| \mathcal{F}(w)$, as extracted from the recoil spectrum in $\bar{B} \rightarrow D^* \ell \bar{\nu}$ decays⁶¹. The line shows a linear fit to the data.

The effect of a positive curvature of the form factor has been investigated by Stone⁶⁴, who finds that the value of $|V_{cb}| \mathcal{F}(1)$ may change by up to +4%. We thus increase the above value by $(2 \pm 2)\%$ and quote the final result as

$$|V_{cb}| \mathcal{F}(1) = (35.3 \pm 1.8) \times 10^{-3}. \quad (57)$$

In future analyses, the extrapolation to zero recoil should be performed including higher-order terms in the expansion (55). It can be shown in a model-independent way that the shape of the form factor is highly constrained by analyticity and unitarity requirements^{65,66}. In particular, the curvature at $w = 1$ is strongly correlated with the slope of the form factor. For the value of \hat{q}^2 given in (56), one obtains a small positive curvature⁶⁶, in agreement with the assumption made in Ref.⁶⁴.

Table 1: Values for $|V_{cb}| \mathcal{F}(1)$ (in units of 10^{-3}) and \hat{q}^2 extracted from measurements of the recoil spectrum in $\bar{B} \rightarrow D^* \ell \bar{\nu}$ decays

	$ V_{cb} \mathcal{F}(1) (10^{-3})$	\hat{q}^2
ARGUS	$38.8 \pm 4.3 \pm 2.5$	$1.17 \pm 0.22 \pm 0.06$
CLEO	$35.1 \pm 1.9 \pm 2.0$	$0.84 \pm 0.12 \pm 0.08$
ALEPH	$31.4 \pm 2.3 \pm 2.5$	$0.39 \pm 0.21 \pm 0.12$
DELPHI	$35.0 \pm 1.9 \pm 2.3$	$0.81 \pm 0.16 \pm 0.10$

Heavy-quark symmetry implies that the general structure of the symmetry-breaking corrections to the form factor at zero recoil is⁵⁸

$$\mathcal{F}(1) = \eta_A \left(1 + 0 \cdot \frac{\Lambda_{\text{QCD}}}{m_Q} + c_2 \frac{\Lambda_{\text{QCD}}^2}{m_Q^2} + \dots \right) \equiv \eta_A (1 + \delta_{1/m^2}), \quad (58)$$

where η_A is a short-distance correction arising from a finite renormalization of the flavour-changing axial current at zero recoil, and δ_{1/m^2} parametrizes second-order (and higher) power corrections. The absence of first-order power corrections at zero recoil is a consequence of Luke’s theorem⁵⁴. The one-loop expression for η_A has been known for a long time^{9,12,67}:

$$\eta_A = 1 + \frac{\alpha_s(M)}{\pi} \left(\frac{m_b + m_c}{m_b - m_c} \ln \frac{m_b}{m_c} - \frac{8}{3} \right) \simeq 0.96. \quad (59)$$

The scale M in the running coupling constant can be fixed by adopting the prescription of Brodsky, Lepage and Mackenzie (BLM)⁶⁸, where it is identified with the average virtuality of the gluon in the one-loop diagrams that contribute to η_A . If $\alpha_s(M)$ is defined in the $\overline{\text{MS}}$ scheme, the result is⁶⁹ $M \simeq 0.51\sqrt{m_c m_b}$. Several estimates of higher-order corrections to η_A have been discussed. A renormalization-group resummation of logarithms of the type $(\alpha_s \ln m_b/m_c)^n$, $\alpha_s(\alpha_s \ln m_b/m_c)^n$ and $m_c/m_b(\alpha_s \ln m_b/m_c)^n$ leads to^{18,70–73} $\eta_A \simeq 0.985$. On the other hand, a resummation of “renormalon-chain” contributions of the form $\beta_0^{n-1}\alpha_s^n$, where $\beta_0 = 11 - \frac{2}{3}n_f$ is the first coefficient of the QCD β -function, gives⁷⁴ $\eta_A \simeq 0.945$. Using these partial resummations to estimate the uncertainty gives $\eta_A = 0.965 \pm 0.020$. Recently, Czarnecki has improved this estimate by calculating η_A at two-loop order⁷⁵. His result,

$$\eta_A = 0.960 \pm 0.007, \quad (60)$$

is in excellent agreement with the BLM-improved one-loop expression (59). Here the error is taken to be the size of the two-loop correction.

The analysis of the power corrections δ_{1/m^2} is more difficult, since it cannot rely on perturbation theory. Three approaches have been discussed: in the “exclusive approach”, all $1/m_Q^2$ operators in the HQET are classified and their matrix elements estimated, leading to^{45,76} $\delta_{1/m^2} = -(3 \pm 2)\%$; the “inclusive approach” has been used to derive the bound $\delta_{1/m^2} < -3\%$, and to estimate that⁷⁷ $\delta_{1/m^2} = -(7 \pm 3)\%$; the “hybrid approach” combines the virtues of the former two to obtain a more restrictive lower bound on δ_{1/m^2} . This leads to⁷⁸

$$\delta_{1/m^2} = -0.055 \pm 0.025. \quad (61)$$

Combining the above results, adding the theoretical errors linearly to be conservative, gives

$$\mathcal{F}(1) = 0.91 \pm 0.03 \quad (62)$$

for the normalization of the hadronic form factor at zero recoil. Thus, the corrections to the heavy-quark limit amount to a moderate decrease of the form factor of about 10%. This can be used to extract from the experimental result (57) the model-independent value

$$|V_{cb}| = (38.8 \pm 2.0_{\text{exp}} \pm 1.2_{\text{th}}) \times 10^{-3}. \quad (63)$$

3.4. Bounds and Predictions for $\widehat{\varrho}^2$

The slope parameter $\widehat{\varrho}^2$ in the expansion of the physical form factor in (55) differs from the slope parameter ϱ^2 of the Isgur–Wise function by corrections that violate the heavy-quark symmetry. The short-distance corrections have been calculated, with the result⁷⁸

$$\widehat{\varrho}^2 = \varrho^2 + (0.16 \pm 0.02) + O(1/m_Q). \quad (64)$$

Bjorken has shown that the slope of the Isgur–Wise function is related to the form factors of transitions of a ground-state heavy meson into excited states, in which the light degrees of freedom carry quantum numbers $j^P = \frac{1}{2}^+$ or $\frac{3}{2}^+$, by a sum rule which is an expression of quark–hadron duality: in the heavy-quark limit, the inclusive sum of the probabilities for decays into hadronic states is equal to the probability for the free quark transition. If one normalizes the latter probability to unity, the sum rule takes the form^{79–81}

$$\begin{aligned} 1 = & \frac{w+1}{2} \left\{ |\xi(w)|^2 + \sum_l |\xi^{(l)}(w)|^2 \right\} \\ & + (w-1) \left\{ 2 \sum_m |\tau_{1/2}^{(m)}(w)|^2 + (w+1)^2 \sum_n |\tau_{3/2}^{(n)}(w)|^2 \right\} + O[(w-1)^2], \end{aligned} \quad (65)$$

where l, m, n label the radial excitations of states with the same spin-parity quantum numbers. The terms in the first line on the right-hand side of the sum rule correspond to transitions into states containing light constituents with quantum numbers $j^P = \frac{1}{2}^-$. The ground state gives a contribution proportional to the Isgur–Wise function, and excited states contribute proportionally to analogous functions $\xi^{(l)}(w)$. Because at zero recoil these states must be orthogonal to the ground state, it follows that $\xi^{(l)}(1) = 0$, and the corresponding contributions to (65) are actually of order $(w-1)^2$. The contributions in the second line correspond to transitions into states with $j^P = \frac{1}{2}^+$ or $\frac{3}{2}^+$. Because of the change in parity, these are p -wave transitions. The amplitudes are proportional to the velocity $|\vec{v}_f| = (w^2 - 1)^{1/2}$ of the final state in the rest frame of the initial state, which explains the suppression factor $(w-1)$ in the decay probabilities. The functions $\tau_j(w)$ are the analogues of the Isgur–Wise function for these transitions⁸⁰. Transitions into excited states with quantum numbers other than the above proceed via higher partial waves and are suppressed by at least a factor $(w-1)^2$.

For $w = 1$, eq. (65) reduces to the normalization condition for the Isgur–Wise function. The Bjorken sum rule is obtained by expanding in powers of $(w-1)$ and keeping terms of first order. Taking into account the definition of the slope parameter, $\xi'(1) = -\varrho^2$, one finds that^{79,80}

$$\varrho^2 = \frac{1}{4} + \sum_m |\tau_{1/2}^{(m)}(1)|^2 + 2 \sum_n |\tau_{3/2}^{(n)}(1)|^2 > \frac{1}{4}. \quad (66)$$

Notice that the lower bound is due to the prefactor $\frac{1}{2}(w+1)$ of the first term in (65) and is of purely kinematic origin. In the analogous sum rule for Λ_Q baryons, this factor is absent, and consequently the slope parameter of the baryon Isgur–Wise function is only subject to the trivial constraint^{53,82} $\varrho^2 > 0$.

Voloshin has derived another sum rule involving the form factors for transitions into excited states, which is the analogue of the “optical sum rule” for the dipole scattering of light in atomic physics. It reads⁸³

$$\frac{m_M - m_Q}{2} = \sum_m E_{1/2}^{(m)} |\tau_{1/2}^{(m)}(1)|^2 + 2 \sum_n E_{3/2}^{(n)} |\tau_{3/2}^{(n)}(1)|^2, \quad (67)$$

where E_j are the excitation energies relative to the mass m_M of the ground-state heavy meson. The important point is that this relation can be combined with the Bjorken sum rule to obtain an upper bound for the slope parameter ϱ^2 :

$$\varrho^2 < \frac{1}{4} + \frac{m_M - m_Q}{2E_{\min}}, \quad (68)$$

where E_{\min} denotes the minimum excitation energy. In the quark model, one expects^c that $E_{\min} \simeq m_M - m_Q$, and one may use this as an estimate to obtain $\varrho^2 < 0.75$.

The above discussion of the sum rules ignores renormalization effects. Both perturbative and non-perturbative corrections to (66) and (68) can be incorporated using the OPE, where one introduces a momentum scale $\mu \sim \text{few} \times \Lambda_{\text{QCD}}$ large enough for $\alpha_s(\mu)$ and power corrections of order $(\Lambda_{\text{QCD}}/\mu)^n$ to be small, but otherwise as small as possible to suppress contributions from excited states⁸⁴. The result is⁸⁵ $\varrho_{\min}^2(\mu) < \varrho^2 < \varrho_{\max}^2(\mu)$, where the boundary values are shown in Fig. 8 as a function of the scale μ . Assuming that the OPE works down to values $\mu \simeq 0.8$ GeV, one obtains rather tight bounds for the slope parameters:

$$0.5 < \varrho^2 < 0.8, \quad 0.5 < \hat{\varrho}^2 < 1.1. \quad (69)$$

The allowed region for $\hat{\varrho}^2$ has been increased in order to account for the unknown $1/m_Q$ corrections in the relation (64). The experimental result given in (56) falls inside this region.

These bounds compare well with theoretical predictions for the slope parameters. QCD sum rules have been used to calculate the slope of the Isgur–Wise function. The results obtained by various authors are $\varrho^2 = 0.84 \pm 0.02$ (Bagan et al.⁸⁶), 0.7 ± 0.1 (Neubert⁸⁷), 0.70 ± 0.25 (Blok and Shifman⁸⁸), and 1.00 ± 0.02 (Narison⁸⁹). The UKQCD Collaboration has presented a lattice calculation of the slope of the form factor $\mathcal{F}(w)$, yielding⁹⁰ $\hat{\varrho}^2 = 0.9_{-0.3}^{+0.2+0.4}$. We stress that the sum-rule bounds in (69) are largely model independent; model calculations in strong disagreement with these bounds should be discarded.

^cStrictly speaking, the lowest excited “state” contributing to the sum rule is $D + \pi$, which has an excitation-energy spectrum with a threshold at m_π . However, this spectrum is broad, so that this contribution will not invalidate the upper bound for ϱ^2 derived here.

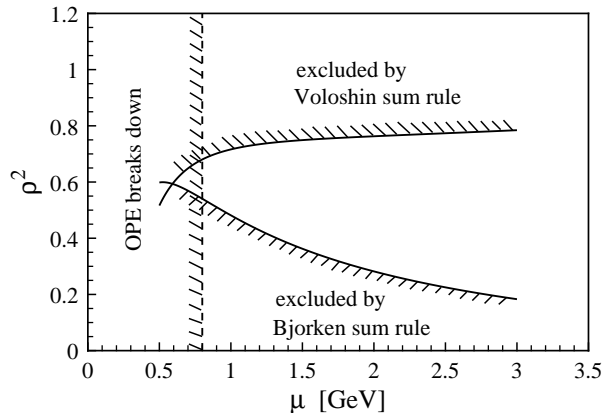


Figure 8: Bounds for the slope parameter ρ^2 following from the Bjorken and Voloshin sum rules.

3.5. Measurement of $\bar{B} \rightarrow D^* \ell \bar{\nu}$ Form Factors

If the lepton mass is neglected, the differential decay distributions in $\bar{B} \rightarrow D^* \ell \bar{\nu}$ decays can be parametrized by three helicity amplitudes, or equivalently by three independent combinations of form factors. It has been suggested that a good choice for three such quantities should be inspired by the heavy-quark limit^{25,91}. One thus defines a form factor $h_{A1}(w)$, which up to symmetry-breaking corrections coincides with the Isgur–Wise function, and two form-factor ratios

$$\begin{aligned} R_1(w) &= \left[1 - \frac{q^2}{(m_B + m_{D^*})^2} \right] \frac{V(q^2)}{A_1(q^2)}, \\ R_2(w) &= \left[1 - \frac{q^2}{(m_B + m_{D^*})^2} \right] \frac{A_2(q^2)}{A_1(q^2)}. \end{aligned} \quad (70)$$

The relation between w and q^2 has been given in (51). This definition is such that in the heavy-quark limit $R_1(w) = R_2(w) = 1$ independently of w .

To extract the functions $h_{A1}(w)$, $R_1(w)$ and $R_2(w)$ from experimental data is a complicated task. However, HQET-based calculations suggest that the w dependence of the form-factor ratios, which is induced by symmetry-breaking effects, is rather mild⁹¹. Moreover, the form factor $h_{A1}(w)$ is expected to have a nearly linear shape over the accessible w range. This motivates to introduce three parameters ρ_{A1}^2 , R_1 and R_2 by

$$\begin{aligned} h_{A1}(w) &\simeq \mathcal{F}(1) \left[1 - \rho_{A1}^2 (w - 1) \right], \\ R_1(w) &\simeq R_1, \\ R_2(w) &\simeq R_2, \end{aligned} \quad (71)$$

where $\mathcal{F}(1) = 0.91 \pm 0.03$ from (62). The CLEO Collaboration has extracted these three parameters from an analysis of the angular distributions in $\bar{B} \rightarrow D^* \ell \bar{\nu}$

decays⁹². The result is:

$$\begin{aligned}\varrho_{A1}^2 &= 0.91 \pm 0.15 \pm 0.06, \\ R_1 &= 1.18 \pm 0.30 \pm 0.12, \\ R_2 &= 0.71 \pm 0.22 \pm 0.07.\end{aligned}\tag{72}$$

Using the HQET, one obtains an essentially model-independent prediction for the symmetry-breaking corrections to R_1 , whereas the corrections to R_2 are somewhat model dependent. To good approximation²⁵

$$\begin{aligned}R_1 &\simeq 1 + \frac{4\alpha_s(m_c)}{3\pi} + \frac{\bar{\Lambda}}{2m_c} \simeq 1.3 \pm 0.1, \\ R_2 &\simeq 1 - \kappa \frac{\bar{\Lambda}}{2m_c} \simeq 0.8 \pm 0.2,\end{aligned}\tag{73}$$

with $\kappa \simeq 1$ from QCD sum rules⁹¹. Here $\bar{\Lambda}$ is the “binding energy” as defined in the mass formula (26). Theoretical calculations^{93,94} as well as phenomenological analyses^{95,96} suggest that $\bar{\Lambda} \simeq 0.45\text{--}0.65$ GeV is the appropriate value to be used in one-loop calculations. A quark-model calculation of R_1 and R_2 gives results similar to the HQET predictions⁹⁷: $R_1 \simeq 1.15$ and $R_2 \simeq 0.91$. The experimental data confirm the theoretical prediction that $R_1 > 1$ and $R_2 < 1$, although the errors are still large.

There is a model-independent relation between the three parameters determined from the analysis of angular distributions and the slope parameter $\widehat{\varrho}^2$ extracted from the semileptonic spectrum. It reads⁷⁸

$$\varrho_{A1}^2 - \widehat{\varrho}^2 = \frac{1}{6} (R_1^2 - 1) + \frac{m_B}{3(m_B - m_{D^*})} (1 - R_2).\tag{74}$$

The CLEO data give 0.07 ± 0.20 for the difference of the slope parameters on the left-hand side, and 0.22 ± 0.18 for the right-hand side. Both values are compatible within errors.

The results of this analysis are very encouraging. Within errors, the experiment confirms the HQET predictions, starting to test them at the level of symmetry-breaking corrections.

3.6. *Decays to Charmless Final States*

For completeness, we will discuss briefly semileptonic B -meson decays into charmless final states, although heavy-quark symmetry does not help much in the analysis of these processes. Recently, the CLEO Collaboration has reported a first signal for the exclusive semileptonic decay modes $\bar{B} \rightarrow \pi \ell \bar{\nu}$ and $\bar{B} \rightarrow \rho \ell \bar{\nu}$. The underlying quark process for these transitions is $b \rightarrow u \ell \bar{\nu}$. Thus, these decays provide information on the strength of the CKM matrix element V_{ub} . The observed branching fractions are⁵:

$$B(\bar{B} \rightarrow \pi \ell \bar{\nu}) = \begin{cases} (1.34 \pm 0.45) \times 10^{-4}; & \text{ISGW,} \\ (1.63 \pm 0.57) \times 10^{-4}; & \text{BSW,} \end{cases}$$

$$B(\bar{B} \rightarrow \rho \ell \bar{\nu}) = \begin{cases} (2.28_{-0.83}^{+0.69}) \times 10^{-4}; & \text{ISGW,} \\ (3.88_{-1.39}^{+1.15}) \times 10^{-4}; & \text{BSW.} \end{cases} \quad (75)$$

There is a significant model dependence in the simulation of the reconstruction efficiencies, for which the models of Isgur et al. (ISGW)⁹⁸ and Bauer et al. (BSW)⁹⁹ have been used.

Table 2: Values for $|V_{ub}/V_{cb}|$ extracted from the CLEO measurement of exclusive semileptonic B decays into charmless final states, taking $|V_{cb}| = 0.040$. An average over the experimental results in (75) is used for all except the ISGW and BSW models, where the numbers corresponding to these models are used. The first error quoted is experimental, the second (when available) is theoretical.

Method	Reference	$\bar{B} \rightarrow \pi \ell \bar{\nu}$	$\bar{B} \rightarrow \rho \ell \bar{\nu}$
QCD sum rules	Narison ¹⁰⁰	$0.159 \pm 0.019 \pm 0.001$	$0.066_{-0.009}^{+0.007} \pm 0.003$
	Ball ¹⁰¹	$0.105 \pm 0.013 \pm 0.011$	$0.094_{-0.012}^{+0.010} \pm 0.016$
	Khodj. & Rückl ¹⁰²	0.085 ± 0.010	—
Lattice QCD	UKQCD ¹⁰³	$0.103 \pm 0.012_{-0.010}^{+0.012}$	—
	APE ¹⁰⁴	$0.084 \pm 0.010 \pm 0.021$	—
pQCD	Li & Yu ¹⁰⁵	0.054 ± 0.006	—
Quark models	BSW ⁹⁹	0.093 ± 0.016	$0.076_{-0.014}^{+0.011}$
	KS ¹⁰⁶	0.088 ± 0.011	$0.056_{-0.007}^{+0.006}$
	ISGW2 ¹⁰⁷	0.074 ± 0.012	$0.079_{-0.014}^{+0.012}$

The theoretical description of these heavy-to-light ($b \rightarrow u$) decays is more model dependent than that for heavy-to-heavy ($b \rightarrow c$) transitions, because heavy-quark symmetry does not help to constrain the relevant hadronic form factors. A variety of calculations for such form factors exists, based on QCD sum rules, lattice gauge theory, perturbative QCD, or quark models. Table 2 contains a summary of values extracted for the ratio $|V_{ub}/V_{cb}|$ from a selection of such calculations. Some approaches are more consistent than others in that the extracted values are compatible for the two decay modes. With few exceptions, the results lie in the range

$$\left| \frac{V_{ub}}{V_{cb}} \right|_{\text{excl}} = 0.06\text{--}0.11, \quad (76)$$

which is in good agreement with the measurement of $|V_{ub}|$ obtained from the end-

point region of the lepton spectrum in inclusive semileptonic decays^{3,4}:

$$\left| \frac{V_{ub}}{V_{cb}} \right|_{\text{incl}} = 0.08 \pm 0.01_{\text{exp}} \pm 0.02_{\text{th}}. \quad (77)$$

Clearly, this is only the first step towards a more reliable determination of $|V_{ub}|$; yet, with the discovery of exclusive $b \rightarrow u$ transitions an important milestone has been met. Efforts must now concentrate on more reliable methods to determine the form factors for heavy-to-light transitions. Some new ideas in this direction have been discussed recently. They are based on lattice calculations¹⁰⁸, analyticity constraints^{109,110}, or variants of the form-factor relations for heavy-to-heavy transitions¹¹¹.

4. Inclusive Decay Rates and Lifetimes

Inclusive decay rates determine the probability of the decay of a particle into the sum of all possible final states with a given set of quantum numbers. An example is provided by the inclusive semileptonic decay rate of the B meson, $\Gamma(\bar{B} \rightarrow X_c \ell \bar{\nu})$, where the final state consists of a lepton–neutrino pair accompanied by any number of hadrons with total charm-quark number $n_c = 1$. Here we shall discuss the theoretical description of inclusive decays of hadrons containing a heavy quark^{112–120}. From the theoretical point of view, such decays have two advantages: first, bound-state effects related to the initial state (such as the “Fermi motion” of the heavy quark inside the hadron) can be accounted for in a systematic way using the heavy-quark expansion, in much the same way as explained in the previous sections; secondly, the fact that the final state consists of a sum over many hadronic channels eliminates bound-state effects related to the properties of individual hadrons. This second feature is based on a hypothesis known as quark–hadron duality, which is an important concept in QCD phenomenology. The assumption of duality is that cross sections and decay rates, which are defined in the physical region (i.e. the region of time-like momenta), are calculable in QCD after a “smearing” or “averaging” procedure has been applied¹²¹. In semileptonic decays, it is the integration over the lepton and neutrino phase space that provides a “smearing” over the invariant hadronic mass of the final state (so-called “global” duality). For non-leptonic decays, on the other hand, the total hadronic mass is fixed, and it is only the fact that one sums over many hadronic states that provides an “averaging” (so-called “local” duality). Clearly, local duality is a stronger assumption than global duality. It is important to stress that quark–hadron duality cannot yet be derived from first principles, although it is a necessary assumption for many applications of QCD. The validity of global duality has been tested experimentally using data on hadronic τ decays¹²². A more formal attempt to address the problem of quark–hadron duality can be found in Ref.¹²³.

Using the optical theorem, the inclusive decay width of a hadron H_b containing

a b quark can be written in the form

$$\Gamma(H_b \rightarrow X) = \frac{1}{2m_{H_b}} 2 \text{Im} \langle H_b | \mathbf{T} | H_b \rangle, \quad (78)$$

where the transition operator \mathbf{T} is given by the time-ordered product of two effective Lagrangians:

$$\mathbf{T} = i \int d^4x T \{ \mathcal{L}_{\text{eff}}(x), \mathcal{L}_{\text{eff}}(0) \}. \quad (79)$$

In fact, inserting a complete set of states inside the time-ordered product, we find the standard expression

$$\Gamma(H_b \rightarrow X) = \frac{1}{2m_{H_b}} \sum_X (2\pi)^4 \delta^4(p_H - p_X) |\langle X | \mathcal{L}_{\text{eff}} | H_b \rangle|^2 \quad (80)$$

for the decay rate. For the case of semileptonic and non-leptonic decays, \mathcal{L}_{eff} is the effective weak Lagrangian given in (4), which in practice is corrected for short-distance effects^{124–128} arising from the exchange of gluons with virtualities between m_W and m_b . If some quantum numbers of the final states X are specified, the sum over intermediate states is restricted appropriately. In the case of the inclusive semileptonic decay rate, for instance, the sum would include only those states X containing a lepton–neutrino pair.

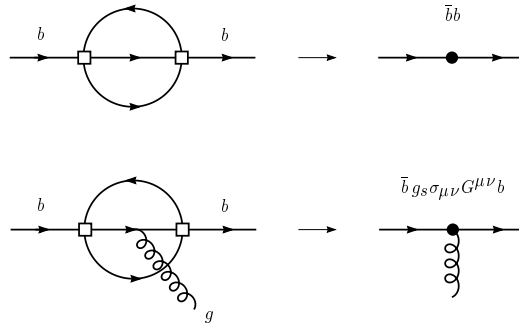


Figure 9: Perturbative contributions to the transition operator \mathbf{T} (left), and the corresponding operators in the OPE (right). The open squares represent a four-fermion interaction of the effective Lagrangian \mathcal{L}_{eff} , while the black circles represent local operators in the OPE.

In perturbation theory, some contributions to the transition operator are given by the two-loop diagrams shown on the left-hand side in Fig. 9. Because of the large mass of the b quark, the momenta flowing through the internal lines in these diagrams are large. It is thus possible to construct an OPE for the transition operator, in which \mathbf{T} is represented as a series of local operators containing the heavy-quark fields. The operator with the lowest dimension, $d = 3$, is $\bar{b}b$. It arises from integrating over the internal lines in the first diagram shown in the figure. The

only gauge-invariant operator with dimension $d = 4$ is $\bar{b} i \not{D} b$; however, the equation of motion implies that between physical states this operator can be replaced by $m_b \bar{b} b$. The first operator that is different from $\bar{b} b$ has dimension $d = 5$ and contains the gluon field. It is given by $\bar{b} g_s \sigma_{\mu\nu} G^{\mu\nu} b$. This operator arises from diagrams in which a gluon is emitted from one of the internal lines, such as the second diagram shown in the figure.

For dimensional reasons, the matrix elements of such higher-dimensional operators are suppressed by inverse powers of the heavy-quark mass. Thus, any inclusive decay rate of a hadron H_b can be written in the form^{113–115}:

$$\Gamma(H_b \rightarrow X_f) = \frac{G_F^2 m_b^5}{192\pi^3} \left\{ c_3^f \langle \bar{b} b \rangle_H + c_5^f \frac{\langle \bar{b} g_s \sigma_{\mu\nu} G^{\mu\nu} b \rangle_H}{m_b^2} + \dots \right\}, \quad (81)$$

where the prefactor arises naturally from the loop integrations, c_n^f are calculable coefficient functions (which also contain the relevant CKM matrix elements) depending on the quantum numbers f of the final state, and $\langle O \rangle_H$ are the (normalized) forward matrix elements of local operators, for which we use the short-hand notation

$$\langle O \rangle_H = \frac{1}{2m_{H_b}} \langle H_b | O | H_b \rangle. \quad (82)$$

In the next step, these matrix elements are systematically expanded in powers of $1/m_b$, using the technology of the HQET. Introducing the velocity-dependent fields b_v of the HQET, where v denotes the velocity of the hadron H_b , one finds^{45,115,116}

$$\begin{aligned} \langle \bar{b} b \rangle_H &= 1 - \frac{\mu_\pi^2(H_b) - \mu_G^2(H_b)}{2m_b^2} + O(1/m_b^3), \\ \langle \bar{b} g_s \sigma_{\mu\nu} G^{\mu\nu} b \rangle_H &= 2\mu_G^2(H_b) + O(1/m_b), \end{aligned} \quad (83)$$

where we have defined the HQET matrix elements

$$\begin{aligned} \mu_\pi^2(H_b) &= \frac{1}{2m_{H_b}} \langle H_b(v) | \bar{b}_v (i\vec{D})^2 b_v | H_b(v) \rangle, \\ \mu_G^2(H_b) &= \frac{1}{2m_{H_b}} \langle H_b(v) | \bar{b}_v \frac{g_s}{2} \sigma_{\mu\nu} G^{\mu\nu} b_v | H_b(v) \rangle. \end{aligned} \quad (84)$$

Here $(i\vec{D})^2 = (iv \cdot D)^2 - (iD)^2$; in the rest frame, this is the square of the operator for the spatial momentum of the heavy quark. Inserting these results into (81), we obtain

$$\Gamma(H_b \rightarrow X_f) = \frac{G_F^2 m_b^5}{192\pi^3} \left\{ c_3^f \left(1 - \frac{\mu_\pi^2(H_b)}{2m_b^2} \right) + (4c_5^f + c_3^f) \frac{\mu_G^2(H_b)}{2m_b^2} + \dots \right\}. \quad (85)$$

It is instructive to understand the appearance of the “kinetic energy” contribution μ_π^2 , which is the gauge-covariant extension of the square of the b -quark momentum inside the heavy hadron. This contribution is the field-theory analogue of the Lorentz factor $(1 - \vec{v}_b^2)^{1/2} \simeq 1 - \vec{p}_b^2/2m_b^2$, in accordance with the fact that the lifetime, $\tau = 1/\Gamma$, for a moving particle increases due to time dilation.

The main result of the heavy-quark expansion for inclusive decay rates is that the free quark decay (i.e. the parton model) provides the first term in a systematic $1/m_b$ expansion, i.e.

$$\Gamma(H_b \rightarrow X_f) = \frac{G_F^2 m_b^5}{192\pi^3} c_3^f \left\{ 1 + O(1/m_b^2) \right\}. \quad (86)$$

For dimensional reasons, the free-quark decay rate is proportional to the fifth power of the b -quark mass. The non-perturbative corrections to this picture, which arise from bound-state effects inside the hadron H_b , are suppressed by (at least) two powers of the heavy-quark mass, i.e. they are of relative order $(\Lambda_{\text{QCD}}/m_b)^2$. Note that the absence of first-order power corrections is a simple consequence of the equation of motion, as there is no independent gauge-invariant operator of dimension $d = 4$ that could appear in the OPE. The fact that bound-state effects in inclusive decays are strongly suppressed explains *a posteriori* the success of the parton model in describing such processes.

The hadronic matrix elements appearing in the heavy-quark expansion (85) can be determined to some extent from the known masses of heavy hadron states. For the B meson, one finds that⁴⁵

$$\begin{aligned} \mu_\pi^2(B) &= -\lambda_1 = (0.4 \pm 0.2) \text{ GeV}^2, \\ \mu_G^2(B) &= 3\lambda_2 = \frac{3}{4} (m_{B^*}^2 - m_B^2) \simeq 0.36 \text{ GeV}^2, \end{aligned} \quad (87)$$

where λ_1 and λ_2 are the parameters appearing in the mass formula (27). For the ground-state baryon Λ_b , in which the light constituents have total spin zero, it follows that

$$\mu_G^2(\Lambda_b) = 0, \quad (88)$$

while the matrix element $\mu_\pi^2(\Lambda_b)$ obeys the relation

$$(m_{\Lambda_b} - m_{\Lambda_c}) - (\overline{m}_B - \overline{m}_D) = \left[\mu_\pi^2(B) - \mu_\pi^2(\Lambda_b) \right] \left(\frac{1}{2m_c} - \frac{1}{2m_b} \right) + O(1/m_Q^2), \quad (89)$$

where \overline{m}_B and \overline{m}_D denote the spin-averaged masses introduced in connection with (37). With the value of m_{Λ_b} given in (35), this leads to

$$\mu_\pi^2(B) - \mu_\pi^2(\Lambda_b) = (0.01 \pm 0.03) \text{ GeV}^2. \quad (90)$$

What remains to be calculated, then, is the coefficient functions c_n^f for a given inclusive decay channel. We shall now discuss the most important applications of this general formalism.

4.1. Determination of $|V_{cb}|$ from Inclusive Semileptonic Decays

The extraction of $|V_{cb}|$ from the inclusive semileptonic decay rate of the B meson is based on the expression^{113–115}

$$\Gamma(\bar{B} \rightarrow X_c \ell \bar{\nu}) = \frac{G_F^2 m_b^5}{192\pi^3} |V_{cb}|^2 \left\{ \left(1 + \frac{\lambda_1 + 3\lambda_2}{2m_b^2} \right) \left[f\left(\frac{m_c}{m_b}\right) + \frac{\alpha_s(M)}{\pi} g\left(\frac{m_c}{m_b}\right) \right] \right\}$$

$$- \frac{6\lambda_2}{m_b^2} \left(1 - \frac{m_c^2}{m_b^2} \right)^4 + \dots \Bigg\}, \quad (91)$$

where m_b and m_c are the poles mass of the b and c quarks (defined to a given order in perturbation theory), and $f(x)$ and $g(x)$ are phase-space functions:

$$f(x) = 1 - 8x^2 + 8x^6 - x^8 - 12x^4 \ln x^2, \quad (92)$$

and $g(x)$ is given elsewhere¹²⁹. The theoretical uncertainties in this determination of $|V_{cb}|$ are quite different from those entering the analysis of exclusive decays. In particular, in inclusive decays there appear the quark masses rather than the meson masses. Moreover, the theoretical description relies on the assumption of global quark–hadron duality, which is not necessary for exclusive decays. One should distinguish three sources of theoretical uncertainties:

Hadronic parameters: The non-perturbative corrections are very small; with $-\lambda_1 = (0.4 \pm 0.2) \text{ GeV}^2$ and $\lambda_2 = 0.12 \text{ GeV}^2$, one finds a reduction of the free-quark decay rate by $-(4.2 \pm 0.5)\%$. The uncertainty in this number is below 1% and thus completely negligible.

Quark-mass dependence: The fact that $\Gamma \sim m_b^5 f(m_c/m_b)$ suggests a strong dependence of the decay rate on the value of the b -quark mass. However, this dependence becomes milder if one chooses m_b and $\Delta m = m_b - m_c$ as independent variables. This is apparent from Fig. 10, which shows that $\Gamma \sim m_b^{2.3} \Delta m^{2.7}$. This choice of variables is also preferred from a conceptual point of view, since it leads to essentially uncorrelated theoretical uncertainties: whereas $m_b = m_B - \bar{\Lambda} + \dots$ is mainly determined by the $\bar{\Lambda}$ parameter of the HQET, the mass difference Δm obeys the expansion shown in (37), i.e. it is sensitive to the kinetic-energy parameter λ_1 . Theoretical uncertainties of 60 MeV on Δm and 200 MeV on m_b are reasonable; values much smaller than this are probably too optimistic. This leads to

$$\left(\frac{\delta\Gamma}{\Gamma} \right)_{\text{masses}} = \sqrt{\left(0.10 \frac{\delta m_b}{200 \text{ MeV}} \right)^2 + \left(0.05 \frac{\delta \Delta m}{60 \text{ MeV}} \right)^2} \simeq 11\%. \quad (93)$$

Perturbative corrections: The perturbative corrections are the most subtle part of the analysis. The semileptonic rate is known exactly to order α_s only¹²⁹, although a partial calculation of the coefficient of order α_s^2 exists¹³⁰. The result is

$$\frac{\Gamma}{\Gamma_{\text{tree}}} = 1 - 1.67 \frac{\alpha_s(m_b)}{\pi} - (1.68\beta_0 + \dots) \left(\frac{\alpha_s(m_b)}{\pi} \right)^2 + \dots \quad (94)$$

The one-loop correction is moderate; it amounts to about -11% . Of the two-loop coefficient, only the part proportional to the β -function coefficient β_0 is known. For $n_f = 3$ light quark flavours, this term gives $1.68\beta_0 \simeq 15.1$, corresponding to a rather

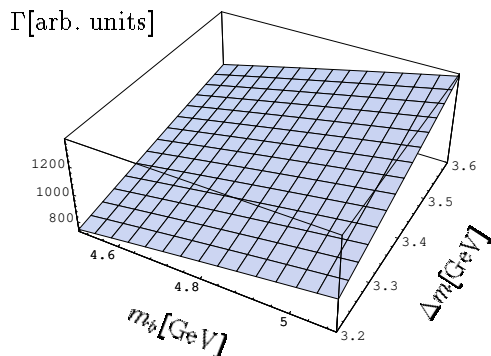


Figure 10: Dependence of the inclusive semileptonic decay rate on m_b and $\Delta m = m_b - m_c$.

large correction of about -6% . One may take this as an estimate of the perturbative uncertainty. The dependence of the result on the choice of the renormalization scale and scheme has been investigated, too, and found to be of order¹³¹ 6% . Yet, the actual perturbative uncertainty may be larger than that. A subset of higher-order corrections, the so-called “renormalon-chain” contributions of the form $\beta_0^{n-1} \alpha_s^n$, can be summed to all orders in perturbation theory, leading to¹³² $\Gamma/\Gamma_{\text{tree}} = 0.77 \pm 0.05$, which is equivalent to choosing the rather low scale $M \simeq 1$ GeV in (91). This estimate is 12% lower than the one-loop result. These considerations show that there are substantial perturbative uncertainties in the calculation of the semileptonic decay rate. They could only be reduced with a complete two-loop calculation, which is however quite a formidable task. At present, we consider $(\delta\Gamma/\Gamma)_{\text{pert}} \simeq 10\%$ a reasonable estimate.

Adding, as previously, the theoretical errors linearly, and taking the square root, leads to

$$\frac{\delta|V_{cb}|}{|V_{cb}|} \simeq 10\% \quad (95)$$

for the theoretical uncertainty in the determination of $|V_{cb}|$ from inclusive decays, keeping in mind that this method relies in addition on the assumption of global quark–hadron duality. Taking the result of Ball et al.¹³² for the central value, we quote

$$|V_{cb}| = (0.0400 \pm 0.0040) \left(\frac{B_{\text{SL}}}{10.9\%} \right)^{1/2} \left(\frac{\tau_B}{1.6 \text{ ps}} \right)^{-1/2}. \quad (96)$$

With the new world averages for the semileptonic branching ratio, $B_{\text{SL}} = (10.90 \pm 0.46)\%$ (see below), and for the average B -meson lifetime⁴⁶, $\tau_B = (1.60 \pm 0.03)$ ps, we obtain

$$|V_{cb}| = (40.0 \pm 0.9_{\text{exp}} \pm 4.0_{\text{th}}) \times 10^{-3}. \quad (97)$$

This is in excellent agreement with the value in (63), which has been extracted from the analysis of the exclusive decay $\bar{B} \rightarrow D^* \ell \bar{\nu}$. This agreement is gratifying

given the differences of the methods used, and it provides an indirect test of global quark–hadron duality. Combining the two measurements gives the final result

$$|V_{cb}| = 0.039 \pm 0.002. \quad (98)$$

After V_{ud} and V_{us} , this is now the third-best known entry in the CKM matrix.

4.2. *Semileptonic Branching Ratio and Charm Counting*

The semileptonic branching ratio of B mesons is defined as

$$B_{\text{SL}} = \frac{\Gamma(\bar{B} \rightarrow X e \bar{\nu})}{\sum_{\ell} \Gamma(\bar{B} \rightarrow X \ell \bar{\nu}) + \Gamma_{\text{NL}} + \Gamma_{\text{rare}}}, \quad (99)$$

where Γ_{NL} and Γ_{rare} are the inclusive rates for non-leptonic and rare decays, respectively. The main difficulty in calculating B_{SL} is not in the semileptonic width, but in the non-leptonic one. As mentioned above, the calculation of non-leptonic decays in the heavy-quark expansion relies on the strong assumption of local quark–hadron duality.

Measurements of the semileptonic branching ratio have been performed by various experimental groups, using both model-dependent and model-independent analyses. The status of the results is controversial, as there is a discrepancy between low-energy measurements performed at the $\Upsilon(4s)$ resonance and high-energy measurements performed at the Z^0 resonance. The average value at low energies is¹³³ $B_{\text{SL}} = (10.37 \pm 0.30)\%$. High-energy measurements performed at LEP, on the other hand, give¹³⁴ $B_{\text{SL}}^{(b)} = (11.11 \pm 0.23)\%$. The superscript (b) indicates that this value refers not to the B meson, but to a mixture of b hadrons (approximately 40% B^- , 40% \bar{B}^0 , 12% B_s , and 8% Λ_b). Assuming that the corresponding semileptonic width $\Gamma_{\text{SL}}^{(b)}$ is close to that of the B meson,^d we can correct for this and find $B_{\text{SL}} = (\tau(B)/\tau(b)) B_{\text{SL}}^{(b)} = (11.30 \pm 0.26)\%$, where $\tau(b) = (1.57 \pm 0.03)$ ps is the average lifetime corresponding to the above mixture of b hadrons⁴⁶. The discrepancy between the low-energy and high-energy measurements of the semileptonic branching ratio is therefore larger than 3 standard deviations. If we take the average and inflate the error to account for this disturbing fact, we obtain

$$B_{\text{SL}} = (10.90 \pm 0.46)\%. \quad (100)$$

In understanding this result, an important aspect is charm counting, i.e. the measurement of the average number n_c of charm hadrons produced per B decay. Recently, two new (preliminary) measurements of this quantity have been performed. The CLEO Collaboration has presented the value^{133,135} $n_c = 1.16 \pm 0.05$, and the ALEPH Collaboration has reported the result¹³⁶ $n_c = 1.20 \pm 0.08$. The average is

$$n_c = 1.17 \pm 0.04. \quad (101)$$

^dTheoretically, this is expected to be a very good approximation.

In the parton model, one finds¹³⁷ $B_{\text{SL}} \simeq 13\%$ and $n_c \simeq 1.15$. Whereas n_c is in agreement with experiment, the semileptonic branching ratio is predicted to be too large. With the establishment of the $1/m_Q$ expansion the non-perturbative corrections to the parton model could be computed, and they turned out to be too small to improve the prediction. This led Bigi et al. to conclude that values $B_{\text{SL}} < 12.5\%$ cannot be accommodated by theory, thus giving rise to a puzzle referred to as the “baffling semileptonic branching ratio”¹³⁸. The situation has changed recently, however, when it was shown that higher-order perturbative corrections lower the value of B_{SL} significantly¹³⁹. The exact order- α_s corrections to the non-leptonic width have been computed for $m_c \neq 0$, and an analysis of the renormalization scale and scheme dependence has been performed. In particular, it turns out that radiative corrections increase the partial width $\Gamma(\bar{B} \rightarrow X_{c\bar{c}s})$ by a large amount. This has two effects: it lowers the semileptonic branching ratio, but at the price of a higher value of n_c .

The original analysis of Bagan et al. has recently been corrected in an erratum¹³⁹. Here we shall present the results of an independent numerical analysis using the same theoretical input (for a detailed discussion, see Ref.¹⁴⁰). The semileptonic branching ratio and n_c depend on the quark-mass ratio m_c/m_b and on the ratio μ/m_b , where μ is the scale used to renormalize the coupling constant $\alpha_s(\mu)$ and the Wilson coefficients appearing in the non-leptonic decay rate. The freedom in choosing the scale μ reflects our ignorance of higher-order corrections, which are neglected when the perturbative expansion is truncated at order α_s . Below we shall consider several choices for the renormalization scale. We allow the pole masses of the heavy quarks to vary in the range [see (39)]

$$m_b = (4.8 \pm 0.2) \text{ GeV}, \quad m_b - m_c = (3.40 \pm 0.06) \text{ GeV}, \quad (102)$$

corresponding to $0.25 < m_c/m_b < 0.33$. Non-perturbative effects appearing at order $1/m_b^2$ in the heavy-quark expansion are described by the single parameter $\lambda_2 \simeq 0.12 \text{ GeV}^2$ defined in (87); the dependence on the parameter λ_1 is the same for all inclusive decay rates and cancels out in B_{SL} and n_c . For the two choices $\mu = m_b$ and $\mu = m_b/2$, we obtain

$$\begin{aligned} B_{\text{SL}} &= \begin{cases} 12.0 \pm 1.0\%; & \mu = m_b, \\ 10.9 \pm 0.9\%; & \mu = m_b/2, \end{cases} \\ n_c &= \begin{cases} 1.21 \mp 0.06; & \mu = m_b, \\ 1.22 \mp 0.06; & \mu = m_b/2. \end{cases} \end{aligned} \quad (103)$$

The uncertainties in the two quantities, which result from the variation of m_c/m_b in the range given above, are anticorrelated. Notice that the semileptonic branching ratio has a stronger scale dependence than n_c . This is illustrated in Fig. 11, which shows the two quantities as a function of μ . By choosing a low renormalization scale, values $B_{\text{SL}} < 12\%$ can easily be accommodated. The experimental data prefer a scale $\mu/m_b \sim 0.5$, which is indeed not unnatural. Using the BLM scale setting

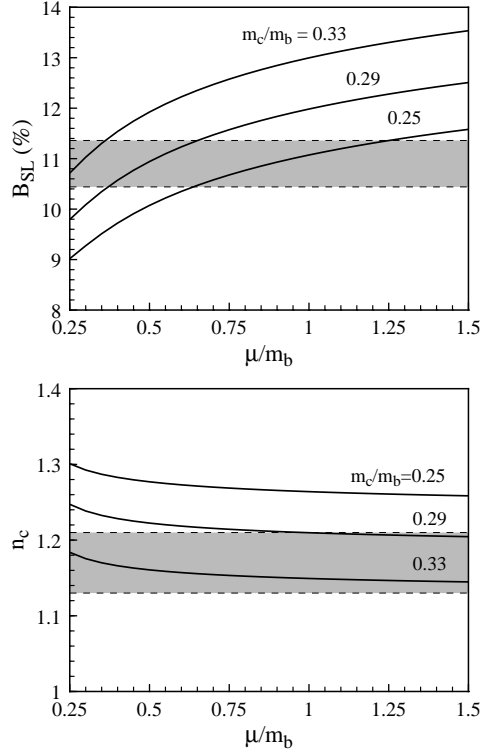


Figure 11: Scale dependence of the theoretical predictions for the semileptonic branching ratio and n_c . The bands show the average experimental values given in (100) and (101).

method⁶⁸, Luke et al. have estimated that $\mu \gtrsim 0.32m_b$ is an appropriate scale in this case¹³⁰.

The combined theoretical predictions for the semileptonic branching ratio and charm counting are shown in Fig. 12. They are compared with the experimental results obtained from low- and high-energy measurements. It was argued that the combination of a low semileptonic branching ratio and a low value of n_c would constitute a potential problem for the Standard Model¹⁴¹. However, with the new experimental and theoretical numbers, only for the low-energy measurements a small discrepancy remains between theory and experiment.

Previous attempts to resolve the “problem of the semileptonic branching ratio” have focused on four possibilities:

- It has been argued that the experimental value of n_c may depend on model assumptions about the production of charm hadrons, which are sometimes questionable^{141,142}.
- It has been pointed out that the assumption of local quark–hadron duality could fail in non-leptonic B decays^{143–146}. If so, this will most likely happen

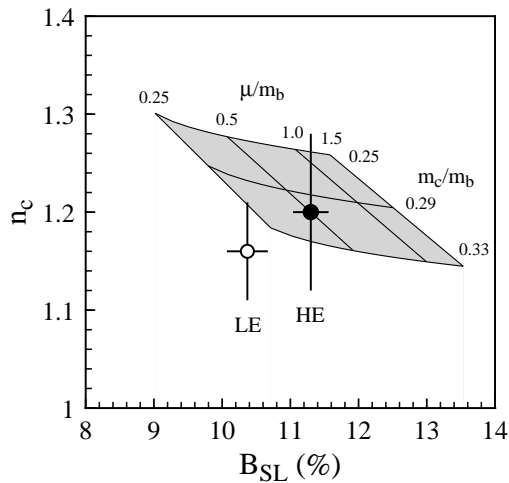


Figure 12: Combined theoretical predictions for the semileptonic branching ratio and charm counting as a function of the quark-mass ratio m_c/m_b and the renormalization scale μ . The data points show the average experimental values for B_{SL} and n_c obtained in low-energy (LE) and high-energy (HE) measurements, as discussed in the text.

in the channel $b \rightarrow c\bar{c}s$, where the energy release, $E = m_B - m_{X(c\bar{c}s)}$, is of order 1.5 GeV or less. However, if one assumes that sizeable duality violations occur only in this channel, it is impossible to improve the agreement between theory and experiment¹⁴⁷.

- Another possibility is that higher-order corrections in the $1/m_b$ expansion, which were previously thought to be negligible, give a sizeable contribution. As will be discussed in more detail below, certain corrections involving the participation of a spectator quark are enhanced by phase space, so that they lead to effects of relative size¹⁴⁷ $16\pi^2(\Lambda_{\text{QCD}}/m_b)^3$ rather than $(\Lambda_{\text{QCD}}/m_b)^3$. They could lower the semileptonic branching ratio by up to 1%, depending on the size of some hadronic matrix elements¹⁴⁰. Lattice calculations could help to confirm or rule out this possibility.
- Finally, there is also the possibility to invoke New Physics^{148–151}. One may, for instance, consider extensions of the Standard Model with enhanced flavour-changing neutral currents such as $b \rightarrow sg$. The effect of such a contribution would be that both B_{SL} and n_c are reduced by a factor $(1 + \eta B_{\text{SL}}^{\text{SM}})^{-1}$, where $\eta = (\Gamma_{\text{rare}} - \Gamma_{\text{rare}}^{\text{SM}})/\Gamma_{\text{SL}}$. To obtain a sizeable decrease requires values $\eta \sim 0.5$, which are large (in the Standard Model, $\Gamma_{\text{rare}}^{\text{SM}}/\Gamma_{\text{SL}} \sim 0.1$), but not excluded by current experiments.

For completeness, we briefly discuss the semileptonic branching ratio for B decays into a τ lepton, which is suppressed by phase space. The ratio of the semileptonic rates for decays into τ leptons and into electrons can be calculated reliably.

The result is¹¹⁸

$$\frac{B(\bar{B} \rightarrow X \tau \bar{\nu}_\tau)}{B(\bar{B} \rightarrow X e \bar{\nu}_\tau)} = 0.22 \pm 0.02. \quad (104)$$

This ratio has been measured at LEP and is found to be¹³³

$$\frac{B(\bar{B} \rightarrow X \tau \bar{\nu}_\tau)}{B(\bar{B} \rightarrow X e \bar{\nu}_\tau)} = 0.234 \pm 0.029, \quad (105)$$

in good agreement with the theoretical prediction.

4.3. Lifetime Ratios of b Hadrons

The heavy-quark expansion shows that the lifetimes of all hadrons containing a b quark agree up to non-perturbative corrections suppressed by at least two powers of $1/m_b$. In particular, it predicts that

$$\begin{aligned} \frac{\tau(B^-)}{\tau(B^0)} &= 1 + O(1/m_b^3), \\ \frac{\tau(B_s)}{\tau(B_d)} &= (1.00 \pm 0.01) + O(1/m_b^3), \\ \frac{\tau(\Lambda_b)}{\tau(B^0)} &= 1 + \frac{\mu_\pi^2(\Lambda_b) - \mu_\pi^2(B)}{2m_b^2} - c_G \frac{\mu_G^2(B)}{m_b^2} + O(1/m_b^3) \\ &\simeq 0.98 + O(1/m_b^3), \end{aligned} \quad (106)$$

where $c_G \simeq 1.1$, and we have used (87) and (90). The uncertainty in the value of the ratio $\tau(B_s)/\tau(B_d)$ arises from unknown SU(3)-violating effects in the matrix elements of B_s mesons. The above theoretical predictions may be compared with the average experimental values for the lifetime ratios, which are^{46,152}:

$$\begin{aligned} \frac{\tau(B^-)}{\tau(B^0)} &= 1.02 \pm 0.04, \\ \frac{\tau(B_s)}{\tau(B_d)} &= 1.01 \pm 0.07, \\ \frac{\tau(\Lambda_b)}{\tau(B^0)} &= 0.78 \pm 0.05. \end{aligned} \quad (107)$$

Whereas the lifetime ratios of the different B mesons are in good agreement with the theoretical prediction, the low value of the lifetime of the Λ_b baryon is surprising.

To understand the structure of the lifetime differences requires to go further in the $1/m_b$ expansion¹⁵³. Although at first sight it appears that higher-order corrections could be safely neglected given the smallness of the $1/m_b^2$ corrections, this impression is erroneous for two reasons: first, at order $1/m_b^3$ in the heavy-quark expansion for non-leptonic decay rates there appear four-quark operators, whose matrix elements explicitly depend on the flavour of the spectator quark(s) in the hadron H_b , and hence are responsible for lifetime differences between hadrons

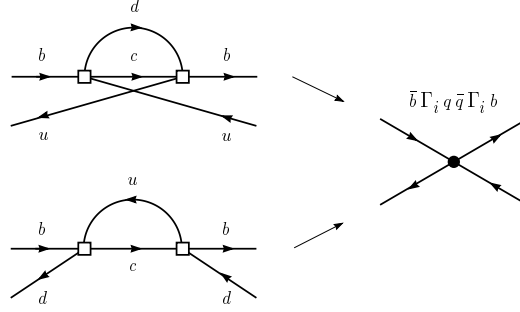


Figure 13: Spectator contributions to the transition operator \mathbf{T} (left), and the corresponding operators in the OPE (right). Here Γ_i denotes some combination of Dirac and colour matrices.

with different light constituents; secondly, these spectator effects receive a phase-space enhancement factor of $16\pi^2$ with respect to the leading terms in the OPE¹⁴⁷. This can be seen from Fig. 13, which shows that the corresponding contributions to the transition operator \mathbf{T} arise from one-loop rather than two-loop diagrams. The presence of this phase-space enhancement factor leads to a peculiar structure of the heavy-quark expansion for non-leptonic rates, which may be displayed as follows:

$$\Gamma = \Gamma_0 \left\{ 1 + x_2 \left(\frac{\Lambda_{\text{QCD}}}{m_b} \right)^2 + x_3 \left(\frac{\Lambda_{\text{QCD}}}{m_b} \right)^3 + \dots \right. \\ \left. + 16\pi^2 \left[y_3 \left(\frac{\Lambda_{\text{QCD}}}{m_b} \right)^3 + y_4 \left(\frac{\Lambda_{\text{QCD}}}{m_b} \right)^4 + \dots \right] \right\}. \quad (108)$$

Here x_n and y_n are coefficients of order unity. It is conceivable that the terms of order $16\pi^2 (\Lambda_{\text{QCD}}/m_b)^3$ could be larger than the ones of order $(\Lambda_{\text{QCD}}/m_b)^2$. It is thus important to include this type of corrections to all predictions for non-leptonic rates. Moreover, there is a challenge to calculate the hadronic matrix elements of the corresponding four-quark operators with high accuracy. Lattice calculations could help to improve the existing estimates of such matrix elements.

In total, a set of four four-quark operators is induced by spectator effects. They are:

$$\begin{aligned} O_{\text{V-A}}^q &= \bar{b} \gamma_\mu (1 - \gamma_5) q \bar{q} \gamma^\mu (1 - \gamma_5) b, \\ O_{\text{S-P}}^q &= \bar{b} (1 - \gamma_5) q \bar{q} (1 + \gamma_5) b, \\ T_{\text{V-A}}^q &= \bar{b} \gamma_\mu (1 - \gamma_5) t_a q \bar{q} \gamma^\mu (1 - \gamma_5) t_a b, \\ T_{\text{S-P}}^q &= \bar{b} (1 - \gamma_5) t_a q \bar{q} (1 + \gamma_5) t_a b, \end{aligned} \quad (109)$$

where q is a light quark, and t_a are the generators of colour SU(3). In most previous analyses of spectator effects the hadronic matrix elements of these operators have been estimated making simplifying assumptions^{153–156}. For the matrix elements

between B -meson states the vacuum saturation approximation¹⁵⁷ was assumed, i.e. the matrix elements of the four-quark operators have been evaluated by inserting the vacuum inside the current products. This leads to

$$\begin{aligned}\langle \bar{B}_q | O_{V-A}^q | \bar{B}_q \rangle &= \langle \bar{B}_q | O_{S-P}^q | \bar{B}_q \rangle = f_{B_q}^2 m_{B_q}^2, \\ \langle \bar{B}_q | T_{V-A}^q | \bar{B}_q \rangle &= \langle \bar{B}_q | T_{S-P}^q | \bar{B}_q \rangle = 0,\end{aligned}\quad (110)$$

where f_{B_q} is the decay constant of the B_q meson, which is defined as

$$\langle 0 | \bar{q} \gamma^\mu \gamma_5 b | \bar{B}_q(v) \rangle = i f_{B_q} m_{B_q} v^\mu. \quad (111)$$

This approach has been criticized by Chernyak¹⁵⁸, who estimates that corrections to the vacuum saturation approximation can be as large as 50%.

An unbiased analysis of spectator effects, which avoids assumptions about hadronic matrix elements, can be performed if instead of (110) one defines¹⁴⁰

$$\begin{aligned}\langle \bar{B}_q | O_{V-A}^q | \bar{B}_q \rangle &= B_1 f_{B_q}^2 m_{B_q}^2, \\ \langle \bar{B}_q | O_{S-P}^q | \bar{B}_q \rangle &= B_1 f_{B_q}^2 m_{B_q}^2, \\ \langle \bar{B}_q | T_{V-A}^q | \bar{B}_q \rangle &= \varepsilon_1 f_{B_q}^2 m_{B_q}^2, \\ \langle \bar{B}_q | T_{S-P}^q | \bar{B}_q \rangle &= \varepsilon_2 f_{B_q}^2 m_{B_q}^2.\end{aligned}\quad (112)$$

The values of the dimensionless hadronic parameters B_i and ε_i are currently not known; ultimately, they may be calculated using some field-theoretic approach such as lattice gauge theory or QCD sum rules. The vacuum saturation approximation corresponds to setting $B_i = 1$ and $\varepsilon_i = 0$ (at some scale μ , where the approximation is believed to be valid). For real QCD, however, it is known that

$$B_i = O(1), \quad \varepsilon_i = O(1/N_c), \quad (113)$$

where N_c is the number of colours. Below, we shall treat B_i and ε_i (renormalized at the scale m_b) as unknown parameters. Similarly, the relevant hadronic matrix elements of the four-quark operators between Λ_b -baryon states can be parametrized by two parameters, \tilde{B} and r , where $\tilde{B} = 1$ in the valence-quark approximation, in which the colour of the quark fields in the operators is identified with the colour of the quarks inside the baryon¹⁴⁰.

4.3.1. Lifetime ratio for B^- and B^0

The lifetimes of the charged and neutral B mesons differ because of two types of spectator effects illustrated in Fig. 14. They are referred to as Pauli interference and W exchange^{154–156}. In the operator language, these effects are represented by the hadronic matrix elements of the local four-quark operators given in (112). In fact, the diagrams in Fig. 14 can be obtained from those in Fig. 13 by cutting the internal lines, which corresponds to taking the imaginary part in (78).

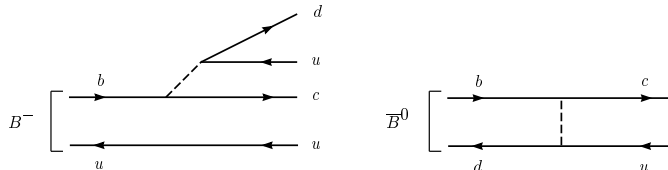


Figure 14: Pauli interference and W exchange contributions to the lifetimes of the B^- and the \bar{B}^0 mesons. The spectator effect in the first diagram arises from the interference due to the presence of two identical \bar{u} quarks in the final state.

The explicit calculation of these spectator effects leads to¹⁴⁰

$$\Delta\Gamma_{\text{spec}}(B_q) = \frac{G_F^2 m_b^5}{192\pi^3} |V_{cb}|^2 16\pi^2 \frac{f_B^2 m_B}{m_b^3} \zeta_{B_q}, \quad (114)$$

where

$$\zeta_{B^-} \simeq -0.4B_1 + 6.6\varepsilon_1, \quad \zeta_{B^0} \simeq -2.2\varepsilon_1 + 2.4\varepsilon_2. \quad (115)$$

Note the factor of $16\pi^2$ in (114), which arises from the phase-space enhancement of spectator effects. Given that the parton-model result for the total decay width is

$$\Gamma_{\text{tot}}(B) \simeq 3.7 \times \frac{G_F^2 m_b^5}{192\pi^3} |V_{cb}|^2, \quad (116)$$

we see that the characteristic scale of spectator contributions is

$$4\pi^2 \frac{f_B^2 m_B}{m_b^3} \simeq \left(\frac{2\pi f_B}{m_b} \right)^2 \simeq 5\%. \quad (117)$$

Thus, it is natural that the lifetimes of different b hadrons differ by a few per cent.

The precise value of the lifetime ratio depends crucially on the size of the hadronic matrix elements. Taking $f_B = 200$ MeV for the decay constant of the B meson (see Ref.²⁵ and references therein), i.e. absorbing the uncertainty in this parameter into the definition of B_i and ε_i , leads to¹⁴⁰

$$\frac{\tau(B^-)}{\tau(B^0)} \simeq 1 + 0.03B_1 - 0.71\varepsilon_1 + 0.20\varepsilon_2. \quad (118)$$

The most striking feature of this result is that the coefficients of the colour-octet operators T_{V-A} and T_{S-P} are orders of magnitude larger than those of the colour-singlet operator O_{V-A} . As a consequence, the vacuum insertion approximation, which was adopted in Ref.¹⁵³ to predict that $\tau(B^-)/\tau(B_d)$ is larger than unity by an amount of order 5%, cannot be trusted. With ε_i of order $1/N_c$, it is conceivable that the non-factorizable contributions actually dominate the result. Thus, without a detailed calculation of the parameters ε_i no reliable prediction can be obtained. Given our present ignorance about the true values of the hadronic matrix elements,

we must conclude that even the sign of the sum of the spectator contributions cannot be predicted. A lifetime ratio in the range $0.8 < \tau(B^-)/\tau(B^0) < 1.2$ could be easily accommodated by theory.

In view of these considerations, the experimental fact that the lifetime ratio turns out to be very close to unity is somewhat of a surprise. It implies a constraint on a certain combination of the colour-octet matrix elements, which reads

$$\varepsilon_1 - 0.3\varepsilon_2 = \text{few } \%. \quad (119)$$

4.3.2. *Lifetime ratio for B_s and B_d*

The lifetimes of the two neutral mesons B_s and B_d differ because spectator effects depend on the flavour of the light quark, and moreover because the hadronic matrix elements in the two cases differ by SU(3) symmetry-breaking corrections. It is difficult to predict the sign of the net effect, but the magnitude cannot be larger than one or two per cent^{140,153}. Hence

$$\frac{\tau(B_s)}{\tau(B_d)} = 1 \pm O(1\%), \quad (120)$$

which is consistent with the experimental value in (107). Note that $\tau(B_s)$ denotes the average lifetime of the two B_s states.

4.3.3. *Lifetime ratio for Λ_b and B^0*

Although, as shown in (106), lifetime differences between heavy mesons and baryons start at order $1/m_b^2$, the main effects are expected to appear at order $1/m_b^3$ in the heavy-quark expansion. However, here one encounters the problem that the matrix elements of four-quark operators are needed between baryon states. Very little is known about such matrix elements. Bigi et al. have adopted a simple non-relativistic quark model and conclude that¹⁵³

$$\frac{\tau(\Lambda_b)}{\tau(B^0)} = 0.90-0.95. \quad (121)$$

An even smaller lifetime difference has been obtained by Rosner¹⁵⁹.

An unbiased analysis gives, in the present case¹⁴⁰:

$$\frac{\tau(\Lambda_b)}{\tau(B^0)} \simeq 0.98 - 0.17\varepsilon_1 + 0.20\varepsilon_2 - (0.013 + 0.022\tilde{B})r, \quad (122)$$

where \tilde{B} and r are expected to be positive and of order unity. Given the structure of this result, it seems difficult to explain the experimental value $\tau(\Lambda_b)/\tau(B^0) = 0.78 \pm 0.05$ without violating the bound (119)^e. Essentially the only possibility is to

^eAnother constraint arises if one does not want to spoil the theoretical prediction for the semileptonic branching ratio¹⁴⁰.

have r of order 2–4 or so, as there are good theoretical arguments why \tilde{B} cannot be much larger than unity. On the other hand, in a constituent quark picture, r is the ratio of the wave functions determining the probability to find a light quark at the location of the b quark inside the Λ_b baryon and the B meson, i.e.

$$r = \frac{|\psi_{bq}^{\Lambda_b}(0)|^2}{|\psi_{bq}^{B^q}(0)|^2}, \quad (123)$$

and it is hard to see how this ratio could be much different from unity.

In view of the above discussion, the problem of the short Λ_b lifetime appears as a puzzle, whose explanation may lie beyond the heavy-quark expansion. If the current experimental value persists, one may have to question the validity of local quark–hadron duality, which is assumed in the theoretical calculation of lifetimes and (non-leptonic) inclusive decay rates.

5. CP Violation

The violation of CP symmetry is one of the most intriguing aspects of high-energy physics. Experimentally, it is one of the least tested properties of the Standard Model. To date, there is only a single unambiguous measurement of a CP-violating parameter: the measurement of ϵ_K in K decays¹⁶⁰. The Standard Model description of CP violation is very predictive, on the other hand; all CP-violating effects are related to the phase δ of the CKM matrix. Yet, this description has two major difficulties: first, CP violation is a necessary prerequisite for baryogenesis¹⁶¹, but CP violation in the Standard Model is believed to be too small to account for the observed baryon asymmetry in the Universe; secondly, there is the so-called strong CP problem. The symmetries of the strong interactions allow a term in the QCD Lagrangian that violates CP:

$$\theta \frac{\alpha_s}{4\pi} \text{Tr} G_{\mu\nu} \tilde{G}^{\mu\nu}. \quad (124)$$

The problem is that such a term would contribute to the electric dipole moment of the neutron^{162,163}. In general, electric dipole moments of elementary particles are sensitive probes of CP-violating effects. Since the only vector that characterizes an elementary particle is its spin,^f we must have $\vec{D} = d\vec{J}$. However, \vec{J} and \vec{D} have different transformation properties under parity and time-reversal transformations. Consequently, if either P or T is a good symmetry, we must have $d = 0$. According to the CPT theorem, a violation of time-reversal symmetry implies CP violation. This is why measurements of electric dipole moments can be used to constrain CP-violating parameters. The current experimental upper bound on the electric dipole moment of the neutron

$$|d_n| < 1.1 \times 10^{-25} e \text{ cm} \quad (95\% \text{ CL}) \quad (125)$$

^fIn this sense, the term “elementary particle” applies to the neutron, too.

implies $|\theta| < 10^{-9}$, corresponding to an extreme fine-tuning of a parameter in the QCD Lagrangian. The above two problems call for extensions of the Standard Model, such as the Peccei–Quinn symmetry¹⁶⁴. The prospects are thus good that detailed studies of CP-violating phenomena at future B factories will provide hints to physics beyond the Standard Model.

Besides measurements of the electric dipole moments of the electron and the neutron, the most interesting observables for CP violation are the weak decays of K and B mesons. In this section, we will present first a general, model-independent discussion and classification of CP-violating effects in meson decays. We will distinguish three types of CP violation: direct CP violation in weak decays, indirect CP violation in the mixing of neutral meson states, and CP violation in the interference of mixing and decay. We will then focus on an analysis of these effects in the Standard Model. A more detailed discussion of CP violation in and beyond the Standard Model can be found in the comprehensive review articles by Nir¹⁶⁵, and by Buchalla et al.¹⁶⁶.

5.1. P , C , and CP Transformations

We start with a discussion of the parity, charge-conjugation and CP transformations acting on meson states. The parity transformation is a space-time transformation, under which $t \rightarrow t$, $\vec{x} \rightarrow -\vec{x}$. It changes the sign of momenta, $\vec{p} \rightarrow -\vec{p}$, leaving spins unchanged. For pseudoscalar mesons P and \bar{P} , the parity transformation implies (adopting the common phase conventions)

$$\mathbf{P} |P(\vec{p})\rangle = -|P(-\vec{p})\rangle, \quad \mathbf{P} |\bar{P}(\vec{p})\rangle = -|\bar{P}(-\vec{p})\rangle. \quad (126)$$

Charge conjugation is a transformation that relates particles and antiparticles, leaving all space-time coordinates unchanged, i.e.

$$\mathbf{C} |P(\vec{p})\rangle = |\bar{P}(\vec{p})\rangle, \quad \mathbf{C} |\bar{P}(\vec{p})\rangle = |P(\vec{p})\rangle. \quad (127)$$

The combined transformation, CP, acts on the pseudoscalar meson states as follows:

$$\mathbf{CP} |P(\vec{p})\rangle = -|\bar{P}(-\vec{p})\rangle, \quad \mathbf{CP} |\bar{P}(\vec{p})\rangle = -|P(-\vec{p})\rangle. \quad (128)$$

For neutral mesons, P^0 and \bar{P}^0 , one can construct the CP eigenstates

$$|P_1^0\rangle = \frac{1}{\sqrt{2}} (|P^0\rangle - |\bar{P}^0\rangle), \quad |P_2^0\rangle = \frac{1}{\sqrt{2}} (|P^0\rangle + |\bar{P}^0\rangle), \quad (129)$$

which obey

$$\mathbf{CP} |P_1^0\rangle = |P_1^0\rangle, \quad \mathbf{CP} |P_2^0\rangle = -|P_2^0\rangle. \quad (130)$$

5.2. Direct CP Violation in Weak Decays

Consider two decay processes related to each other by a CP transformation. Let P and \bar{P} be CP-conjugated pseudoscalar meson states, and f and \bar{f} some CP-conjugated final states:

$$\mathbf{CP} |P\rangle = e^{i\varphi_P} |\bar{P}\rangle, \quad \mathbf{CP} |f\rangle = e^{i\varphi_f} |\bar{f}\rangle. \quad (131)$$

The phases φ_P and φ_f are arbitrary. The CP-conjugated decay amplitudes, A and \bar{A} , can then be written as

$$\begin{aligned} A &= \langle f | \mathcal{H} | P \rangle = \sum_i A_i e^{i\delta_i} e^{i\phi_i}, \\ \bar{A} &= \langle \bar{f} | \mathcal{H} | \bar{P} \rangle = e^{i(\varphi_P - \varphi_f)} \sum_i A_i e^{i\delta_i} e^{-i\phi_i}, \end{aligned} \quad (132)$$

where \mathcal{H} is the effective Hamiltonian for weak decays, and A_i are real partial amplitudes. Two types of phases may appear in the decay amplitudes: the weak phases ϕ_i are parameters of the Lagrangian that violate CP. They usually appear in the electroweak sector of the theory and enter A and \bar{A} with opposite signs. The strong phases δ_i appear in scattering amplitudes even if the Lagrangian is CP invariant. They usually arise from rescattering effects due to the strong interactions and enter A and \bar{A} with the same sign.

Although the definition of strong and weak phases is to a large degree convention dependent, one can show that the ratio

$$\left| \frac{\bar{A}}{A} \right| = \left| \frac{\sum_i A_i e^{i\delta_i} e^{i\phi_i}}{\sum_i A_i e^{i\delta_i} e^{-i\phi_i}} \right| \quad (133)$$

is independent of phase conventions and therefore physically meaningful. The condition

$$\left| \frac{\bar{A}}{A} \right| \neq 1 \quad \Rightarrow \quad \text{direct CP violation} \quad (134)$$

implies CP violation, which results from the interference of decay amplitudes leading to the same final state. Note that this requires at least two partial amplitudes that differ in both their weak and strong phases.

Experimental observation of direct CP violation: Since mixing is unavoidable in neutral meson decays, it is best to observe direct CP violation in the decays of charged mesons. One defines the CP asymmetry:

$$a_f = \frac{\Gamma(P^+ \rightarrow f) - \Gamma(P^- \rightarrow \bar{f})}{\Gamma(P^+ \rightarrow f) + \Gamma(P^- \rightarrow \bar{f})} = \frac{1 - |\bar{A}/A|^2}{1 + |\bar{A}/A|^2}. \quad (135)$$

The requirement of at least two partial amplitudes with different phases forces us to consider non-leptonic decays, since leptonic and semileptonic decays are usually dominated by a single diagram. Non-leptonic decays, on the other hand, can receive so-called “tree” and “penguin”^g contributions³⁴. Penguin diagrams contain a W -boson–quark loop and typically involve other weak phases than tree diagrams. In order to get large interference effects, one needs partial amplitudes with similar

^gIt is a challenge to draw a penguin diagram in such a way that it would actually deserve its name. Among the various rumours about the origin of the name “penguin”, the author tends to believe the one of a well-known CERN theorist, who had a bet that he could introduce any name he wanted into high-energy physics.

magnitude¹⁶⁷. A possibility is to consider decays in which the tree contribution is suppressed, with respect to the penguin contribution, by small CKM parameters. This compensates for the loop suppression of penguin diagrams. In the Standard Model, an example of this type is the decay $B^\pm \rightarrow K^\pm \rho^0$ shown in Fig. 15, for which the tree diagram is proportional to the small CKM parameters $|V_{ub}V_{us}^*| \sim 10^{-3}$, whereas the penguin diagram is proportional to $(\alpha_s/12\pi) \ln(m_t^2/m_b^2) |V_{tb}V_{ts}^*| \simeq 0.02 \times 0.04 \sim 10^{-3}$. Another possibility is to consider tree-forbidden decays, which can only proceed through penguin diagrams. In this case, it is the possibility to have different quarks in the loop (t, c, u) that leads to the interference. Examples are $B^\pm \rightarrow K^\pm K$ and $B^\pm \rightarrow K^\pm \phi$, as well as the radiative decays $B^\pm \rightarrow K^{*\pm} \gamma$ and $B^\pm \rightarrow \rho^\pm \gamma$, see Fig. 16. Unfortunately, the decays $K^\pm \rightarrow \pi^\pm \pi^0$ and $B^\pm \rightarrow \pi^\pm \pi^0$ are pure $\Delta I = \frac{3}{2}$ transitions and are thus governed by a single strong phase δ_2 corresponding to a $\pi\pi$ final state with isospin $I = 2$; isospin $I = 1$ is not allowed because of Bose symmetry. It follows that $a_{\pi\pi} = 0$. There is no unambiguous experimental evidence for direct CP violation yet.

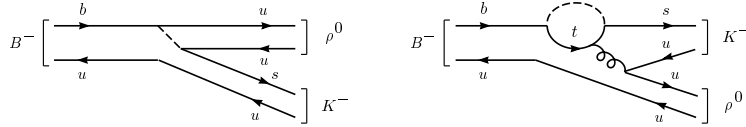


Figure 15: Tree and penguin diagrams for the decay $B^\pm \rightarrow K^\pm \rho^0$.

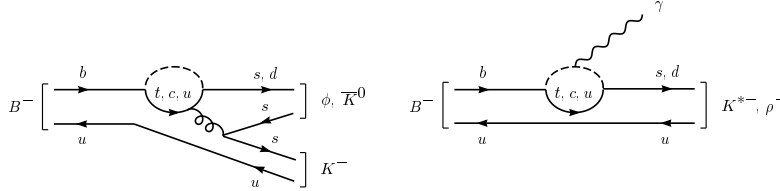


Figure 16: Penguin diagrams for some tree-forbidden B decays.

Hadronic uncertainties: Calculations of direct CP-violating asymmetries have large theoretical uncertainties. They are limited by our incapacity to calculate hadronic matrix elements of quark operators with high accuracy. Moreover, direct CP violation requires non-trivial strong phase shifts, which are notoriously hard to calculate. In some cases, however, part of the uncertainty can be eliminated using isospin analysis^{168–172}.

5.3. Indirect CP Violation in the Mixing of Neutral Mesons

The neutral mesons P^0 and \bar{P}^0 can mix via common decay channels:

$$P^0 \leftrightarrow X \leftrightarrow \bar{P}^0. \quad (136)$$

An arbitrary neutral meson state can thus be written as a superposition of the flavour eigenstates, $a|P^0\rangle + b|\bar{P}^0\rangle$, which obeys the time-dependent Schrödinger equation

$$i\frac{d}{dt}\begin{pmatrix} a \\ b \end{pmatrix} = \mathbf{H}\begin{pmatrix} a \\ b \end{pmatrix} = \left(\mathbf{M} - \frac{i}{2}\mathbf{\Gamma}\right)\begin{pmatrix} a \\ b \end{pmatrix}, \quad (137)$$

where \mathbf{M} and $\mathbf{\Gamma}$ are Hermitian 2×2 matrices, which are called the mass and decay matrices, respectively. Since the Hamilton operator, \mathbf{H} , is not Hermitian, its eigenvectors

$$|P_{1,2}\rangle = p|P^0\rangle \pm q|\bar{P}^0\rangle; \quad |p|^2 + |q|^2 = 1 \quad (138)$$

are not orthogonal, and the eigenvalues

$$\mu_i = M_i - \frac{i}{2}\Gamma_i; \quad i = 1, 2 \quad (139)$$

are complex. This reflects that the states P_1 and P_2 are resonances, not elementary particles. M_i are the masses of these resonances, and Γ_i are their decay widths. The states P_i have a diagonal time evolution given by

$$|P_i(t)\rangle = e^{-iM_i t} e^{-\frac{1}{2}\Gamma_i t} |P_i(0)\rangle. \quad (140)$$

One can show that the ratio

$$\left|\frac{q}{p}\right|^2 = \left|\frac{M_{12}^* - \frac{i}{2}\Gamma_{12}^*}{M_{12} - \frac{i}{2}\Gamma_{12}}\right| \quad (141)$$

is independent of phase conventions and therefore physically meaningful. The condition

$$\left|\frac{q}{p}\right| \neq 1 \quad \Rightarrow \quad \text{indirect CP violation} \quad (142)$$

implies CP violation, which results from the fact that the flavour eigenstates are different from the CP eigenstates.

Let us collect some useful equations related to the mixing of neutral mesons. Define the mass difference $\Delta m = m_2 - m_1$ and the width difference $\Delta\Gamma = \Gamma_2 - \Gamma_1$. Then the following relations hold:

$$\begin{aligned} (\Delta m)^2 - \frac{1}{4}(\Delta\Gamma)^2 &= 4|M_{12}|^2 - |\Gamma_{12}|^2, \\ \Delta m \cdot \Delta\Gamma &= 4\text{Re}(M_{12}\Gamma_{12}^*), \\ \frac{q}{p} &= -\frac{1}{2}\frac{\Delta m - \frac{i}{2}\Delta\Gamma}{M_{12} - \frac{i}{2}\Gamma_{12}} = -2\frac{M_{12}^* - \frac{i}{2}\Gamma_{12}^*}{\Delta m - \frac{i}{2}\Delta\Gamma}. \end{aligned} \quad (143)$$

An alternative common notation is to define $\bar{\epsilon}$ such that

$$p = \frac{1 + \bar{\epsilon}}{\sqrt{2(1 + |\bar{\epsilon}|^2)}}, \quad q = \frac{1 - \bar{\epsilon}}{\sqrt{2(1 + |\bar{\epsilon}|^2)}}, \quad \frac{q}{p} = \frac{1 - \bar{\epsilon}}{1 + \bar{\epsilon}}. \quad (144)$$

q/p in the kaon system: One defines the “short-lived” and “long-lived” neutral kaon states $K_S = K_1$ and $K_L = K_2$, which differ significantly in their lifetimes: $\tau_S = (8.926 \pm 0.012) \times 10^{-11}$ s and $\tau_L = (5.17 \pm 0.04) \times 10^{-8}$ s. Experimentally,

$$\begin{aligned}\Delta m_K &= m_L - m_S = (3.510 \pm 0.018) \times 10^{-15} \text{ GeV}, \\ \Delta\Gamma_K &= \Gamma_L - \Gamma_S = -(7.361 \pm 0.010) \times 10^{-15} \text{ GeV},\end{aligned}\quad (145)$$

so that

$$\Delta\Gamma_K \simeq -2\Delta m_K. \quad (146)$$

If we define

$$\frac{\Gamma_{12}^*}{M_{12}^*} = - \left| \frac{\Gamma_{12}}{M_{12}} \right| e^{i\phi_{12}}, \quad (147)$$

the experimental observation that there is only a small CP violation in the kaon system is reflected in the fact that $|\phi_{12}| = O(10^{-3})$. From (143), we find to first order in this small angle

$$\left(\frac{q}{p} \right)_K \simeq \frac{\Gamma_{12}^*}{|\Gamma_{12}|} \left\{ 1 - i\phi_{12} \frac{1 + i(\frac{\Delta\Gamma_K}{2\Delta m_K})}{1 + (\frac{\Delta\Gamma_K}{2\Delta m_K})^2} \right\}, \quad (148)$$

so that with (146)

$$\left| \frac{q}{p} \right|_K - 1 \simeq -2 \text{Re} \bar{\epsilon}_K \simeq -\phi_{12} = O(10^{-3}). \quad (149)$$

q/p in the B -meson system: Decay channels common to B^0 and \bar{B}^0 , which are responsible for the difference $\Delta\Gamma_B$, are known to have branching fractions of order 10^{-3} or less. Hence, although $\Delta\Gamma_B$ has not yet been measured directly, it follows that $|\Delta\Gamma_B|/\Gamma_B < 10^{-2}$. The observed B^0 - \bar{B}^0 mixing rate implies¹⁷³ $\Delta m_B/\Gamma_B = 0.74 \pm 0.04$, on the other hand, so that model independently

$$|\Delta\Gamma_B| \ll \Delta m_B. \quad (150)$$

Thus, there is a negligible lifetime difference between the CP eigenstates, and one therefore refers to these states as “light” and “heavy”, $B_L = B_1$ and $B_H = B_2$. It follows that $|\Gamma_{12}| \ll |M_{12}|$, and to first order in Γ_{12}/M_{12} we obtain from (143)

$$\left(\frac{q}{p} \right)_B \simeq - \frac{M_{12}^*}{|M_{12}|} \left(1 - \frac{1}{2} \text{Im} \frac{\Gamma_{12}}{M_{12}} \right). \quad (151)$$

Hence

$$\left| \frac{q}{p} \right|_B - 1 \simeq -2 \text{Re} \bar{\epsilon}_B = O(10^{-2}). \quad (152)$$

As in the kaon system, CP violation in B^0 - \bar{B}^0 mixing is a small effect.

Experimental observation of indirect CP violation in the kaon system:

One uses the fact that the semileptonic decays of neutral mesons are flavour-tagging, i.e. $P^0 \not\rightarrow \ell^- \nu$ and $\bar{P}^0 \not\rightarrow \ell^+ \bar{\nu}$, and defines

$$A = \langle \ell^+ \bar{\nu} X | \mathcal{H} | P^0 \rangle, \quad A^* = \langle \ell^- \nu X | \mathcal{H} | \bar{P}^0 \rangle. \quad (153)$$

Because of the large lifetime difference between the two neutral kaon states, it is possible to prepare a beam of K_L particles and to measure the asymmetry

$$a_{\text{SL}}^K = \frac{\Gamma(K_L \rightarrow \ell^+ \bar{\nu} X) - \Gamma(K_L \rightarrow \ell^- \nu X)}{\Gamma(K_L \rightarrow \ell^+ \bar{\nu} X) + \Gamma(K_L \rightarrow \ell^- \nu X)}. \quad (154)$$

Using that $|K_L\rangle = p|K^0\rangle - q|\bar{K}^0\rangle$, and hence

$$\langle \ell^+ \bar{\nu} X | \mathcal{H} | K_L \rangle = pA, \quad \langle \ell^- \nu X | \mathcal{H} | K_L \rangle = -qA^*, \quad (155)$$

we find that

$$a_{\text{SL}}^K = \frac{1 - |q/p|^2}{1 + |q/p|^2} = \frac{2 \operatorname{Re} \bar{\epsilon}_K}{1 + |\bar{\epsilon}_K|^2} \simeq 2 \operatorname{Re} \bar{\epsilon}_K. \quad (156)$$

Experimentally, it was found that

$$a_{\text{SL}}^K = (3.27 \pm 0.12) \times 10^{-3}. \quad (157)$$

This was the observation of indirect CP violation in the kaon system¹⁶⁰.

Experimental observation of indirect CP violation in the B-meson system:

Since B_L and B_H have almost identical lifetimes, it is not possible to produce selectively beams of B_L or B_H particles. With $m_{H,L} = m_B \pm \frac{1}{2} \Delta m_B$ and $\Gamma_{H,L} \simeq \Gamma_B$, eq. (140) gives for the time evolution of an initially pure B^0 state:

$$\begin{aligned} |B^0(0)\rangle &= \frac{1}{2p} \left(|B_H\rangle + |B_L\rangle \right), \\ |B^0(t)\rangle &= \frac{1}{2p} e^{-im_B t} e^{-\frac{1}{2}\Gamma_B t} \left\{ e^{-\frac{i}{2}\Delta m_B t} |B_H\rangle + e^{\frac{i}{2}\Delta m_B t} |B_L\rangle \right\} \\ &= e^{-im_B t} e^{-\frac{1}{2}\Gamma_B t} \left\{ \cos\left(\frac{1}{2}\Delta m_B t\right) |B^0\rangle + \frac{iq}{p} \sin\left(\frac{1}{2}\Delta m_B t\right) |\bar{B}^0\rangle \right\}. \end{aligned} \quad (158)$$

Similarly:

$$|\bar{B}^0(t)\rangle = e^{-im_B t} e^{-\frac{1}{2}\Gamma_B t} \left\{ \cos\left(\frac{1}{2}\Delta m_B t\right) |\bar{B}^0\rangle + \frac{ip}{q} \sin\left(\frac{1}{2}\Delta m_B t\right) |B^0\rangle \right\}. \quad (159)$$

Defining the semileptonic asymmetry as

$$a_{\text{SL}}^B = \frac{\Gamma(\bar{B}^0(t) \rightarrow \ell^+ \bar{\nu} X) - \Gamma(B^0(t) \rightarrow \ell^- \nu X)}{\Gamma(\bar{B}^0(t) \rightarrow \ell^+ \bar{\nu} X) + \Gamma(B^0(t) \rightarrow \ell^- \nu X)}, \quad (160)$$

and taking into account that $B^0 \not\rightarrow \ell^- \nu$ and $\bar{B}^0 \not\rightarrow \ell^+ \bar{\nu}$, we obtain

$$a_{\text{SL}}^B = \frac{1 - |q/p|^4}{1 + |q/p|^4} \simeq 4 \operatorname{Re} \bar{\epsilon}_B = O(10^{-2}). \quad (161)$$

To date, there is no experimental evidence for indirect CP violation in the B -meson system.

Hadronic uncertainties: The calculation of $|q/p|$ involves hadronic matrix elements of local four-quark operators (so-called B parameters). The theoretical uncertainty in the calculation of such matrix elements is about 30%.

5.4. *CP Violation in the Interference of Mixing and Decay*

Consider decays of neutral mesons into CP eigenstates:

$$A = \langle f_{\text{CP}} | \mathcal{H} | P^0 \rangle, \quad A^* = \langle f_{\text{CP}} | \mathcal{H} | \bar{P}^0 \rangle. \quad (162)$$

It can be shown that the product

$$\lambda = \frac{q}{p} \cdot \frac{\bar{A}}{A} \quad (163)$$

is independent of phase conventions and thus physically meaningful. In other words, the convention dependence of q/p cancels against that of \bar{A}/A . The condition

$$\lambda \neq 1 \quad \Rightarrow \quad \text{CP violation} \quad (164)$$

implies CP violation. Note that direct CP violation ($|\bar{A}/A| \neq 1$) and indirect CP violation ($|q/p| \neq 1$) imply $|\lambda| \neq 1$, but they are not necessary for the weaker condition $\lambda \neq 1$. In fact, the case $|\lambda| = 1$ but $\operatorname{Im} \lambda \neq 0$ is the theoretically favoured situation. In that case λ is a pure phase, which can be calculated without hadronic uncertainties.

Many decays of neutral B mesons are of the kind described above. If one defines the CP asymmetry^{174–176}

$$a_{f_{\text{CP}}} = \frac{\Gamma(B^0(t) \rightarrow f_{\text{CP}}) - \Gamma(\bar{B}^0(t) \rightarrow f_{\text{CP}})}{\Gamma(B^0(t) \rightarrow f_{\text{CP}}) + \Gamma(\bar{B}^0(t) \rightarrow f_{\text{CP}})} \quad (165)$$

and takes into account that $|q/p|_B \simeq 1$, it follows that

$$a_{f_{\text{CP}}} \simeq \frac{(1 - |\lambda|^2) \cos(\Delta m_B t) - 2 \operatorname{Im} \lambda \sin(\Delta m_B t)}{1 + |\lambda|^2} \xrightarrow{|\lambda|=1} -\operatorname{Im} \lambda \sin(\Delta m_B t). \quad (166)$$

The “clean modes” with $|\lambda| \simeq 1$ are those dominated by a single weak phase ϕ , so that

$$\frac{\bar{A}}{A} \simeq e^{-2i\phi} \quad (167)$$

is close to a pure phase. Examples of such decays are discussed in detail below. Unfortunately, this method is not useful in kaon decays, since

$$\text{Im } \lambda(K \rightarrow \pi\pi) = O(10^{-3}), \quad (168)$$

i.e. very small.

5.5. CP Violation in the Standard Model

We will now specify the general framework described above and discuss CP violation in the context of the Standard Model. Below mass scales of order $m_W \sim 80$ GeV, the Standard Model gauge group $SU_C(3) \times SU_L(2) \times U_Y(1)$ is spontaneously broken to $SU_C(3) \times U_{\text{em}}(1)$, since the scalar Higgs doublet ϕ acquires a vacuum expectation value. This gives masses to the W and Z bosons, as well as to the quarks and leptons. The quark masses arise from the Yukawa couplings to the Higgs doublet, which in the unbroken theory are assumed to be of the most general form invariant under local gauge transformations. The Yukawa interactions are written in terms of the weak eigenstates q' of the quark fields, which have simple transformation properties under $SU_L(2) \times U_Y(1)$. After the symmetry breaking, one redefines the quark fields so as to obtain the mass terms in the canonical form. This has an interesting effect on the form of the flavour-changing charged-current interactions. In the weak basis, these interactions have the form

$$\mathcal{L}_{\text{int}} = -\frac{g}{\sqrt{2}} (\bar{u}'_L, \bar{c}'_L, \bar{t}'_L) \gamma^\mu \begin{pmatrix} d'_L \\ s'_L \\ b'_L \end{pmatrix} W_\mu^\dagger + \text{h.c.} \quad (169)$$

In terms of the mass eigenstates q , however, this becomes

$$\mathcal{L}_{\text{int}} = -\frac{g}{\sqrt{2}} (\bar{u}_L, \bar{c}_L, \bar{t}_L) \gamma^\mu V_{\text{CKM}} \begin{pmatrix} d_L \\ s_L \\ b_L \end{pmatrix} W_\mu^\dagger + \text{h.c.} \quad (170)$$

The CKM mixing matrix V_{CKM} is a unitary matrix in flavour space. In the general case of n quark generations, V_{CKM} would be an $n \times n$ matrix.

For two generations, the mixing matrix can be parametrized by one angle and three phases:

$$\begin{aligned} V &= \begin{pmatrix} \cos \theta_C e^{i\alpha} & \sin \theta_C e^{i\beta} \\ -\sin \theta_C e^{i\gamma} & \cos \theta_C e^{i(\beta+\gamma-\alpha)} \end{pmatrix} \\ &= \begin{pmatrix} e^{i\alpha} & 0 \\ 0 & e^{i\gamma} \end{pmatrix} \begin{pmatrix} \cos \theta_C & \sin \theta_C \\ -\sin \theta_C & \cos \theta_C \end{pmatrix} \begin{pmatrix} 1 & 0 \\ 0 & e^{i(\beta-\alpha)} \end{pmatrix}. \end{aligned} \quad (171)$$

The phases are not observable, however, as they can be absorbed into a redefinition of the phases of the quark fields u_L , c_L , s_L relative to d_L . After this redefinition, the matrix takes the standard form due to Cabibbo¹⁷⁷:

$$V_C = \begin{pmatrix} \cos \theta_C & \sin \theta_C \\ -\sin \theta_C & \cos \theta_C \end{pmatrix}. \quad (172)$$

In the case of three generations, V_{CKM} can be parametrized by three Euler angles and six phases, five of which can be removed by adjusting the relative phases of the left-handed quark fields. Hence, three angles θ_{ij} and one observable phase δ remain in the quark mixing matrix, as was first pointed out by Kobayashi and Maskawa¹⁷⁸. For completeness, we note that in the general case of n generations, it is easy to show that there are $\frac{1}{2}n(n-1)$ angles and $\frac{1}{2}(n-1)(n-2)$ observable phases¹⁷⁹. Therefore, whereas the Cabibbo matrix is real and has only one parameter, the CKM matrix is complex and can be parametrized by four quantities. The imaginary part of the mixing matrix is necessary to describe CP violation in the Standard Model. In general, CP is violated in flavour-changing decays if there is no degeneracy of any two quark masses, and if the quantity $J_{\text{CP}} \neq 0$, where

$$J_{\text{CP}} = |\text{Im}(V_{ij}V_{kl}V_{il}^*V_{kj}^*)|; \quad i \neq k, \quad j \neq l. \quad (173)$$

It can be shown that all CP-violating amplitudes in the Standard Model are proportional to J_{CP} , and that this quantity is invariant under phase redefinitions of the quark fields¹⁸⁰.

Ignoring the strong CP problem, i.e. assuming that $\theta = 0$ in (124), the complex phase of the CKM matrix is the only parameter in the Standard Model that violates CP symmetry. Hence, the Standard Model is very predictive in describing CP-violating effects: all CP-violating observables are in principle calculable in terms of only one parameter. In practice, however, strong interaction effects have to be controlled before such calculations can be performed.

Let us mention two of the most convenient parametrizations of the CKM matrix. The ‘‘standard parametrization’’¹⁸¹ recommended by the Particle Data Group is

$$V_{\text{CKM}} = \begin{pmatrix} c_{12}c_{13} & s_{12}c_{13} & s_{13}e^{-i\delta} \\ -s_{12}c_{23} - c_{12}s_{23}s_{13}e^{i\delta} & c_{12}c_{23} - s_{12}s_{23}s_{13}e^{i\delta} & s_{23}c_{13} \\ s_{12}s_{23} - c_{12}c_{23}s_{13}e^{i\delta} & -c_{12}s_{23} - s_{12}c_{23}s_{13}e^{i\delta} & c_{23}c_{13} \end{pmatrix}. \quad (174)$$

Here, the short-hand notation $c_{ij} = \cos\theta_{ij}$ and $s_{ij} = \sin\theta_{ij}$ is used. Some advantages of this parametrization are the following ones:

- $|V_{ub}| = s_{13}$ is given by a single angle, which experimentally turns out to be very small.
- Because of this, several other entries are given by single angles to an accuracy of better than four digits. They are: $V_{ud} \simeq c_{12}$, $V_{us} \simeq s_{12}$, $V_{cb} \simeq s_{23}$, and $V_{tb} \simeq c_{23}$.
- The CP-violating phase δ appears together with the small parameter s_{13} , making it explicit that CP violation in the Standard Model is a small effect. Indeed, one finds

$$J_{\text{CP}} = |s_{13}s_{23}s_{12}s_{\delta}c_{13}^2c_{23}c_{12}|. \quad (175)$$

For many purposes and applications, it is more convenient to use an approximate parametrization of the CKM matrix, which makes explicit the strong hierarchy

observed experimentally. Setting $c_{13} = 1$ (experimentally, it is known that $c_{13} > 0.99998$) and neglecting s_{13} compared with terms of order unity, we find

$$V_{\text{CKM}} \simeq \begin{pmatrix} c_{12} & s_{12} & s_{13} e^{-i\delta} \\ -s_{12} c_{23} & c_{12} c_{23} & s_{23} \\ s_{12} s_{23} - c_{12} c_{23} s_{13} e^{i\delta} & -c_{12} s_{23} & c_{23} \end{pmatrix}. \quad (176)$$

Now denote $\lambda = s_{12} \simeq 0.22$. Experiments indicate that $s_{23} = O(\lambda^2)$ and $s_{13} = O(\lambda^3)$. Hence, it is natural to define $s_{23} = A \lambda^2$ and $s_{13} e^{-i\delta} = A \lambda^3(\rho - i\eta)$, with A , ρ and η of order unity. An expansion in powers of λ then leads to the Wolfenstein parametrization¹⁸²

$$V_{\text{CKM}} \simeq \begin{pmatrix} 1 - \frac{\lambda^2}{2} & \lambda & A \lambda^3(\rho - i\eta) \\ -\lambda & 1 - \frac{\lambda^2}{2} & A \lambda^2 \\ A \lambda^3(1 - \rho - i\eta) & -A \lambda^2 & 1 \end{pmatrix} + O(\lambda^4). \quad (177)$$

It nicely exhibits the hierarchy of the mixing matrix: the entries on the diagonal are close to unity, V_{us} and V_{cd} are of order 20%, V_{cb} and V_{ts} are of order 4%, and V_{ub} and V_{td} are of order 1% and thus the smallest entries in the matrix. Some care has to be taken when one wants to calculate the quantity J_{CP} in the Wolfenstein parametrization, since the result is of order λ^6 and thus beyond the accuracy of the approximation. However, taking $i = u$, $j = d$, $k = t$, and $l = b$ in (173), we obtain the correct answer

$$J_{\text{CP}} \simeq A^2 \eta \lambda^6 \simeq 1.1 \times 10^{-4} A^2 \eta, \quad (178)$$

which shows that J_{CP} is generically of order 10^{-4} for $\lambda \simeq 0.22$.

In principle, the entries in the first two rows of the mixing matrix are accessible in so-called direct (tree-level) processes, i.e. in weak decays of hadrons containing the corresponding quarks. In practice, $|V_{ud}|$ and $|V_{us}|$ are known to an accuracy of better than 1%, $|V_{cb}|$ is known to 5%, and $|V_{cd}|$ and $|V_{cs}|$ are known to about 10–20%. Hence, the two Wolfenstein parameters λ and A are rather well determined experimentally:

$$\lambda = |V_{us}| = 0.2205 \pm 0.0018, \quad A = \left| \frac{V_{cb}}{V_{us}^2} \right| = 0.80 \pm 0.04. \quad (179)$$

On the other hand, $|V_{ub}|$ has an uncertainty of about 30%, and the same is true for $|V_{td}|$, which is obtained from B^0 – \bar{B}^0 mixing. This implies a rather significant uncertainty in the values of the Wolfenstein parameters ρ and η . A more precise determination of these parameters will be a challenge to experiments and theory over the next decade.

5.6. The Unitarity Triangle

A simple but beautiful way to visualize the implications of unitarity is provided by the so-called unitarity triangle¹⁸³, which uses the fact that the unitarity equation

$$V_{ij} V_{ik}^* = 0 \quad (j \neq k) \quad (180)$$

can be represented as the equation of a closed triangle in the complex plane. There are six such triangles, all of which have the same area¹⁸⁴

$$|A_\Delta| = \frac{1}{2} J_{\text{CP}}. \quad (181)$$

Under phase reparametrizations of the quark fields, the triangles change their orientation in the complex plane, but their shape remains unaffected.

Most useful from the phenomenological point of view is the triangle relation

$$V_{ud}V_{ub}^* + V_{cd}V_{cb}^* + V_{td}V_{tb}^* = 0, \quad (182)$$

since it contains the most poorly known entries in the CKM matrix. It has been widely discussed in the literature^{183–190}. In the standard parametrization, $V_{cd}V_{cb}^*$ is real, and the unitarity triangle has the form shown in Fig. 17. It is useful to rescale the triangle by dividing all sides by $V_{cd}V_{cb}^*$. The rescaled triangle has the coordinates $(0, 0)$, $(1, 0)$, and $(\bar{\rho}, \bar{\eta})$, where¹⁹¹

$$\bar{\rho} = \left(1 - \frac{\lambda^2}{2}\right) \rho, \quad \bar{\eta} = \left(1 - \frac{\lambda^2}{2}\right) \eta \quad (183)$$

are related to the Wolfenstein parameters ρ and η appearing in (177). Unitarity amounts to the statement that the triangle is closed, and CP is violated when the area of the triangle does not vanish, i.e. when all the angles are different from zero.

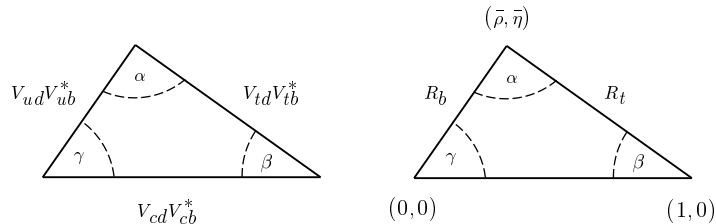


Figure 17: The unitarity triangle (left), and its rescaled form in the $\bar{\rho}$ – $\bar{\eta}$ plane (right). The angle γ coincides with the phase δ of the standard parametrization.

To determine the shape of the triangle, one can aim for measurements of the two sides R_b and R_t , and of the angles α , β , and γ . So far, experimental information is available only on the sides of the triangle. The current value of $|V_{ub}|$ in (77) implies

$$R_b = \sqrt{\bar{\rho}^2 + \bar{\eta}^2} = \left(1 - \frac{\lambda^2}{2}\right) \frac{1}{\lambda} \left| \frac{V_{ub}}{V_{cb}} \right| = 0.35 \pm 0.09. \quad (184)$$

To determine R_t , one needs information on $|V_{td}|$, which can be extracted from B^0 – \bar{B}^0 mixing. In the Standard Model, the mass difference Δm_B between the two neutral meson states is calculable from the box diagrams shown in Fig. 18. The resulting theoretical expression is

$$\Delta m_B = \frac{G_F^2 m_W^2}{6\pi^2} \eta_B B_B f_B^2 m_B S(m_t/m_W) |V_{td}V_{tb}^*|^2, \quad (185)$$

where $\eta_B = 0.55 \pm 0.01$ accounts for the QCD corrections¹⁹², and $S(m_t/m_W)$ is a function of the top quark mass^{193,194}. The product $B_B f_B^2$ parametrizes the hadronic matrix element of a local four-quark operator between B -meson states. There exists a vast literature on calculations of the decay constant f_B and the B_B parameter. Combining the results of some recent QCD sum-rule^{94,195} and lattice calculations^{196–199}, we quote the value

$$f_B = 185 \pm 40 \text{ MeV}. \quad (186)$$

Together with the prediction $B_B \simeq 1.08$ obtained from lattice calculations²⁰⁰, this gives

$$B_B^{1/2} f_B = (200 \pm 40) \text{ MeV}. \quad (187)$$

Solving then (185) for $|V_{td}|$, one obtains²⁰¹

$$|V_{td}| = 8.53 \times 10^{-3} \left(\frac{200 \text{ MeV}}{B_B^{1/2} f_B} \right) \left(\frac{170 \text{ GeV}}{\bar{m}_t(m_t)} \right)^{0.76} \left(\frac{\Delta m_B}{0.465 \text{ ps}^{-1}} \right)^{1/2}. \quad (188)$$

Taking $\bar{m}_t(m_t) = (170 \pm 15) \text{ GeV}$ for the running top-quark mass, and using the average experimental value¹⁷³

$$\Delta m_B = (0.465 \pm 0.024) \text{ ps}^{-1}, \quad (189)$$

gives

$$|V_{td}| = (8.53 \pm 1.81) \times 10^{-3}. \quad (190)$$

The corresponding range of values for R_t is

$$R_t = \sqrt{(1 - \bar{\rho})^2 + \bar{\eta}^2} = \frac{1}{\lambda} \left| \frac{V_{td}}{V_{cb}} \right| = 0.99 \pm 0.22. \quad (191)$$

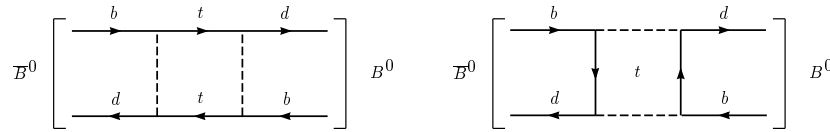


Figure 18: Box diagrams for B^0 - \bar{B}^0 mixing in the Standard Model.

Equations (184) and (191) yield constraints on the Wolfenstein parameters $\bar{\rho}$ and $\bar{\eta}$, which have the form of rings centred at $(\bar{\rho}, \bar{\eta}) = (0, 0)$ and $(0, 1)$. Another constraint can be obtained from the measurement of indirect CP violation in the kaon system. The experimental result on the parameter ϵ_K measuring CP violation in K^0 - \bar{K}^0 mixing implies that the unitarity triangle lies in the upper half plane. The constraint arising in the $\bar{\rho}$ - $\bar{\eta}$ plane has the form of a hyperbola, the shape of which depends on a hadronic parameter B_K . The theoretical prediction is²⁰¹

$$\bar{\eta} \left[(1 - \bar{\rho}) A^2 \left(\frac{m_t}{m_W} \right)^{1.52} + (0.69 \pm 0.05) \right] A^2 B_K \simeq 0.50, \quad (192)$$

where $A = 0.80 \pm 0.04$ according to (179). In the last few years, theoretical calculations of the B_K parameter have converged and give results in the ballpark of

$$B_K = 0.75 \pm 0.15. \quad (193)$$

In particular, the most recent lattice calculations^{202,203} are in good agreement with the results obtained using the $1/N_c$ expansion^{204,205}, and the differences with previous, lower predictions for B_K based on duality and chiral symmetry^{206,207} have been understood.

In principle, the measurement of the ratio $\text{Re}(\epsilon'/\epsilon)$ in the kaon system could provide a determination of η independent of ρ . In practice, however, the experimental situation is unclear^{208,209}, and the theoretical calculations^{210–212} of this ratio are affected by large uncertainties, so that there currently is no useful bound to be derived.

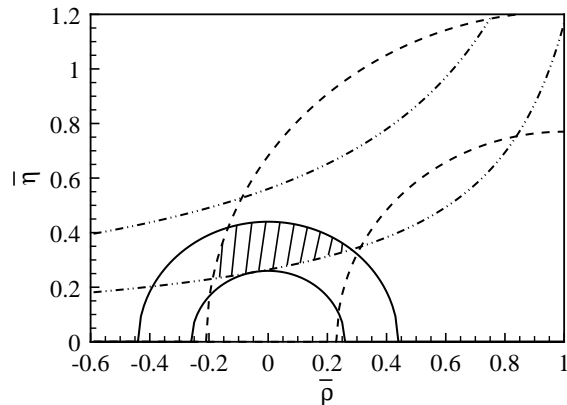


Figure 19: Experimental constraints on the unitarity triangle in the $\bar{\rho}$ - $\bar{\eta}$ plane. The region between the solid (dashed) circles is allowed by the measurement of R_b (R_t) discussed above. The dash-dotted curves show the constraint following from the measurement of the ϵ_K parameter in the kaon system. The shaded region shows the allowed range for the tip of the unitarity triangle. The base of the triangle has the coordinates $(0,0)$ and $(1,0)$.

In Fig. 19, we show the constraints which the measurements of R_b , R_t , and ϵ_K imply in the $\bar{\rho}$ - $\bar{\eta}$ plane. Given the present theoretical and experimental uncertainties in the analysis of charmless B decays, B^0 - \bar{B}^0 mixing, and CP violation in the kaon system, there is still a rather large region allowed for the Wolfenstein parameters. This has important implications. For instance, the allowed region for the angle β of the unitarity triangle (see Fig. 17) is such that

$$0.34 < \sin 2\beta < 0.75. \quad (194)$$

Below, we will discuss that the CP asymmetry in the decay $\bar{B} \rightarrow \psi K_S$, which is one of the favoured modes to search for CP violation at a future B factory, is proportional to $\sin 2\beta$. Obviously, the prospects for discovering CP violation with such a machine depend on whether $\sin 2\beta$ is closer to the upper or lower bound in (194). A more reliable determination of the shape of the unitarity triangle is thus of great importance.

On the other hand, our knowledge of the unitarity triangle has already improved a lot in the last few years, and we are now reaching a state where the analysis described in this section becomes a serious test of the Standard Model. If the three bands in Fig. 19 did not overlap, this would be an indication of New Physics.

5.7. CP Asymmetries in Neutral B-Meson Decays

As mentioned above, decays of neutral B mesons into CP eigenstates provide for largely model-independent determinations of the angles of the unitarity triangle. In the B -meson system, up to corrections of order 10^{-2} , we have

$$\left(\frac{q}{p}\right)_B \simeq -\frac{M_{12}^*}{|M_{12}|} = \frac{(V_{tb}^*V_{td})^2}{|V_{tb}^*V_{td}|^2} = \frac{V_{tb}^*V_{td}}{V_{tb}V_{td}^*} = e^{-2i\beta}. \quad (195)$$

This combination of CKM parameters can be read off directly from the vertices of the box diagrams in Fig. 18, which in the Standard Model are responsible for the non-diagonal element M_{12}^* of the mass matrix. Notice that for the real part of the box diagrams, which determines M_{12} , the contributions of c and u quarks in the loops can be neglected.

To eliminate hadronic uncertainties, one has to choose decay modes dominated by a single diagram. However, most channels receive contributions from “tree” and “penguin” diagrams, which for a generic $b \rightarrow q \bar{q}' q'$ decay contribute in the ratio^{213–215}

$$\frac{\text{penguin}}{\text{tree}} \sim \frac{\alpha_s}{12\pi} \ln \frac{m_t^2}{m_b^2} \cdot r \cdot \frac{V_{tb}V_{tq}^*}{V_{q'b}V_{q'q}^*}. \quad (196)$$

The first factor arises from the loop suppression of the penguin diagrams and is of order 2%, the second factor accounts for the fact that hadronic matrix elements of penguin operators are usually enhanced with respect to those of the operators appearing in tree diagrams by $r \sim 2$ –5, and the last factor is the ratio of CKM matrix elements.

It follows that there are three possibilities to obtain the dominance of a single diagram:

- If the CKM parameters of the penguin diagram are not enhanced with respect to the tree diagram, i.e. if

$$\left| \frac{V_{tb}V_{tq}^*}{V_{q'b}V_{q'q}^*} \right| \leq 1, \quad (197)$$

the tree diagram dominates over the penguin diagram. Examples of such decays are $\bar{B} \rightarrow \pi\pi$, $\bar{B} \rightarrow D\bar{D}$, $B_s \rightarrow \rho K_S$ and $B_s \rightarrow \psi K_S$.

- If tree diagrams are forbidden, the penguin diagram dominates. Examples of such decays are $\bar{B} \rightarrow \phi K_S$, $\bar{B} \rightarrow K_S K_S$, $B_s \rightarrow \eta' \eta'$ and $B_s \rightarrow \phi K_S$.
- If

$$\arg\left(\frac{V_{tb}V_{tq}^*}{V_{q'b}V_{q'q}^*}\right) = 0 \text{ or } \pi, \quad (198)$$

both the tree and the penguin diagram have the same weak phase. In that case one still has $|\bar{A}/A| = 1$, i.e. no hadronic uncertainties. Examples of such decays are $\bar{B} \rightarrow \phi K_S$ and $B_s \rightarrow \psi \phi$.

Let us illustrate these three classes of decays with explicit examples.

5.7.1. Tree-dominant decays: $\bar{B} \rightarrow \pi\pi$

The decay $\bar{B} \rightarrow \pi\pi$ proceeds through the quark decay $b \rightarrow u\bar{u}d$, for which both the tree and the penguin diagram have CKM parameters of order λ^3 , as shown in Fig. 20. Thus, the tree diagram is dominant, and to a good approximation

$$\lambda_{\pi\pi} = \frac{q}{p} \cdot \frac{\bar{A}}{A} \simeq \frac{V_{tb}^*V_{td}}{V_{tb}V_{td}^*} \cdot \frac{V_{ub}V_{ud}^*}{V_{ub}^*V_{ud}} = e^{-2i\beta} e^{-2i\gamma} = e^{2i\alpha}, \quad (199)$$

and

$$\text{Im } \lambda_{\pi\pi} \simeq \sin 2\alpha. \quad (200)$$

Hadronic uncertainties arise from the small admixture of penguin contributions, which lead to $|\lambda| \neq 1$. They are expected¹⁶⁵ to be of order 10%, and can be reduced further by using isospin analysis^{168–172}.

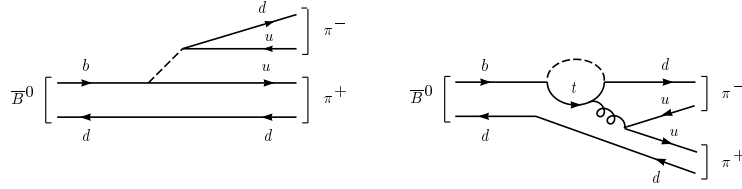


Figure 20: Tree and penguin diagrams for the decay $\bar{B} \rightarrow \pi\pi$.

5.7.2. Tree-forbidden decays: $\bar{B} \rightarrow \phi K_S$

The decay $\bar{B} \rightarrow \phi K_S$ proceeds through the quark transition $b \rightarrow s\bar{s}s$, i.e. it involves a flavour-changing neutral current, which is forbidden at the tree level in the Standard Model. Thus, the relevant diagram is the penguin transition shown in Fig. 21. A new ingredient is the presence of K - \bar{K} mixing, which adds a factor

$$\left(\frac{q}{p}\right)_K \simeq \frac{V_{cs}V_{cd}^*}{V_{cs}^*V_{cd}} \quad (201)$$

in the definition of λ . This is essential for decays with a single K_S , since only $B^0 \rightarrow K^0$ and $\bar{B}^0 \rightarrow \bar{K}^0$ transitions are allowed, and interference between them is possible only due to K - \bar{K} mixing. It follows that

$$\lambda_{\phi K_S} = \left(\frac{q}{p}\right)_B \cdot \left(\frac{q}{p}\right)_K \cdot \frac{\bar{A}}{A} \simeq \frac{V_{tb}^* V_{td}}{V_{tb} V_{td}^*} \cdot \frac{V_{cs} V_{cd}^*}{V_{cs}^* V_{cd}} \cdot \frac{V_{tb} V_{ts}^*}{V_{tb}^* V_{ts}} = e^{-2i\beta}, \quad (202)$$

and therefore

$$\text{Im } \lambda_{\phi K_S} \simeq -\sin 2\beta. \quad (203)$$

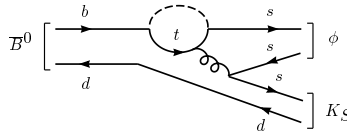


Figure 21: Penguin diagram for the decay $\bar{B} \rightarrow \phi K_S$.

5.7.3. Decays with a single weak phase: $\bar{B} \rightarrow \psi K_S$

The decay $\bar{B} \rightarrow \psi K_S$ is based on the quark transition $b \rightarrow c\bar{c}s$, for which the tree diagram is dominant. As shown in Fig. 22, the tree amplitude is proportional to $V_{cb}V_{cs}^* \sim \lambda^2$. One finds

$$\lambda_{\psi K_S} = -\left(\frac{q}{p}\right)_B \cdot \left(\frac{q}{p}\right)_K \cdot \frac{\bar{A}}{A} \simeq \frac{V_{tb}^* V_{td}}{V_{tb} V_{td}^*} \cdot \frac{V_{cs} V_{cd}^*}{V_{cs}^* V_{cd}} \cdot \frac{V_{cb} V_{cs}^*}{V_{cb}^* V_{cs}} = -e^{-2i\beta}, \quad (204)$$

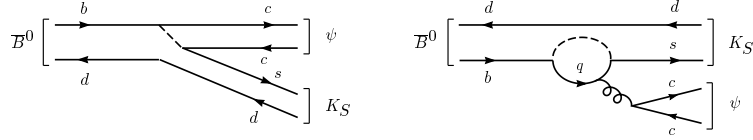
and therefore

$$\text{Im } \lambda_{\psi K_S} \simeq \sin 2\beta. \quad (205)$$

In the present case, the contamination from the penguin contribution is extremely small¹⁷⁵. Depending on the flavour q of the quark in the loop, the penguin contributions are proportional to $V_{tb}V_{ts}^* \simeq \lambda^2$ (for $q = t$), $V_{cb}V_{cs}^* \simeq \lambda^2$ (for $q = c$), and $V_{ub}V_{us}^* \simeq \lambda^4$ (for $q = u$). Because of the relation $V_{tb}V_{ts}^* = -V_{cb}V_{cs}^* + O(\lambda^4)$, it follows that up to very small corrections the penguin contributions have the same weak phase as the tree diagram. Hence, their presence affects neither $|\lambda|$ nor $\text{Im}\lambda$. Detailed estimates show that the hadronic uncertainties are only of order 10^{-3} . This makes the measurement of $\sin 2\beta$ in $\bar{B} \rightarrow \psi K_S$ the theoretically cleanest determination of any CKM parameter. For this reason, this decay is often considered the “gold-plated” mode of a B factory.

The above-mentioned examples are only meant to illustrate the range of possibilities for performing model-independent measurements of CP-violating CKM parameters in neutral B -meson decays into CP eigenstates. A summary and some more examples are given in Table 3. The angle β' appearing in the CP asymmetries for B_s -meson decays is the analogue of the angle β in the unitarity triangle defined by the relation

$$V_{us}V_{ub}^* + V_{cs}V_{cb}^* + V_{ts}V_{tb}^* = 0. \quad (206)$$

Figure 22: Tree and penguin diagrams for the decay $\bar{B} \rightarrow \psi K_S$.Table 3: Examples of CP asymmetries for B and B_s decays into CP eigenstates

Quark decay	B decays		B_s decays	
	Final state	SM prediction	Final state	SM prediction
$b \rightarrow c\bar{c}s$	ψK_S	$-\sin 2\beta$	$D_s^+ D_s^-$	$-\sin 2\beta'$
$b \rightarrow c\bar{c}d$	$D^+ D^-$	$-\sin 2\beta$	ψK_S	$-\sin 2\beta'$
$b \rightarrow u\bar{u}d$	$\pi^+ \pi^-$	$\sin 2\alpha$	ρK_S	$-\sin 2(\gamma + \beta')$
$b \rightarrow s\bar{s}s$	ϕK_S	$-\sin 2(\beta - \beta')$	$\eta' \eta'$	0
$b \rightarrow s\bar{s}d$	$K_S K_S$	0	ϕK_S	$\sin 2(\beta - \beta')$

Experimentally, $|\sin 2\beta'| < 0.06$.

At the end of this section, let us stress again that the Standard Model description of CP violation is at the same time very predictive (since all CP violation is related to a single parameter) and most likely wrong (because of the problems with baryogenesis and strong CP violation). Thus, the prospects are good that once the various CP asymmetries in B -meson decays can be explored at a B factory, deviations from the picture described here will arise. Those deviations would indicate New Physics beyond the Standard Model.

6. Concluding Remarks

We have presented a review of the theory and phenomenology of heavy-flavour physics. The theoretical tools that allow to perform quantitative calculations in this area are the heavy-quark symmetry, the heavy-quark effective theory, and the $1/m_Q$ expansion. We have discussed in detail exclusive weak decays of B mesons, inclusive decay rates and lifetimes of b hadrons, and CP violation in B -meson decays. Besides presenting the status of the latest developments in these fields, our hope was to convince the reader that heavy-flavour physics is a rich and diverse area of research, which is at present characterized by a fruitful interplay between theory and experiments. This has led to many significant discoveries and developments on both sides. Heavy-quark physics has the potential to determine many important parameters of the electroweak theory and to test the Standard Model at low energies.

At the same time, it provides an ideal laboratory to study the nature of non-perturbative phenomena in QCD, still one of the least understood properties of the Standard Model. The phenomenon of CP violation, finally, is one of the most intriguing aspects of high-energy physics. Today, there is only a single unambiguous measurement of a CP-violating quantity. But already in a few years, when CP violation in the B -meson system can be explored at the B factories, this will very likely provide some clues about the physics beyond the Standard Model.

Indeed, the prospects for further significant developments in the field of heavy-flavour physics look rather promising. With the approval of the first asymmetric B factories at SLAC and KEK, with ongoing B -physics programs at the existing facilities at Cornell, Fermilab and CERN, and with plans for future B physics at HERA-B and the LHC-B, there are Beautiful times ahead of us!

Acknowledgements: I am grateful to Irinel Caprini, Maria Girone and Chris Sachrajda for useful discussions and collaboration on some of the subjects presented here, and to Patricia Ball for exchanges concerning the calculation of the semileptonic branching ratio.

1. C. Albajar et al. (UA1 Collaboration), Phys. Lett. B **186**, 247 (1987).
2. H. Albrecht et al. (ARGUS Collaboration), Phys. Lett. B **192**, 245 (1987).
3. H. Albrecht et al. (ARGUS Collaboration), Phys. Lett. B **234**, 409 (1990); **255**, 297 (1991).
4. R. Fulton et al. (CLEO Collaboration), Phys. Rev. Lett. **64**, 16 (1990);
J. Bartelt et al. (CLEO Collaboration), Phys. Rev. Lett. **71**, 4111 (1993).
5. R. Ammar et al. (CLEO Collaboration), conference paper CLEO CONF 95-09 (1995) [eps0165].
6. R. Ammar et al. (CLEO Collaboration), Phys. Rev. Lett. **71**, 674 (1993).
7. M.S. Alam et al. (CLEO Collaboration), Phys. Rev. Lett. **74**, 2885 (1995).
8. E.V. Shuryak, Phys. Lett. B **93**, 134 (1980); Nucl. Phys. B **198**, 83 (1982).
9. J.E. Paschalis and G.J. Gounaris, Nucl. Phys. B **222**, 473 (1983);
F.E. Close, G.J. Gounaris, and J.E. Paschalis, Phys. Lett. B **149**, 209 (1984).
10. S. Nussinov and W. Wetzel, Phys. Rev. D **36**, 130 (1987).
11. M.B. Voloshin and M.A. Shifman, Yad. Fiz. **45**, 463 (1987) [Sov. J. Nucl. Phys. **45**, 292 (1987)].
12. M.B. Voloshin and M.A. Shifman, Yad. Fiz. **47**, 801 (1988) [Sov. J. Nucl. Phys. **47**, 511 (1988)].
13. N. Isgur and M.B. Wise, Phys. Lett. B **232**, 113 (1989); **237**, 527 (1990).
14. E. Eichten and F. Feinberg, Phys. Rev. D **23**, 2724 (1981).
15. W.E. Caswell and G.P. Lepage, Phys. Lett. B **167**, 437 (1986).
16. E. Eichten, in: Field Theory on the Lattice, edited by A. Billoire et al., Nucl. Phys. B (Proc. Suppl.) **4**, 170 (1988).
17. G.P. Lepage and B.A. Thacker, in: Field Theory on the Lattice, edited by A. Billoire et al., Nucl. Phys. B (Proc. Suppl.) **4**, 199 (1988).
18. H.D. Politzer and M.B. Wise, Phys. Lett. B **206**, 681 (1988); **208**, 504 (1988).
19. E. Eichten and B. Hill, Phys. Lett. B **234**, 511 (1990); **243**, 427 (1990).
20. B. Grinstein, Nucl. Phys. B **339**, 253 (1990).
21. H. Georgi, Phys. Lett. B **240**, 447 (1990).
22. A.F. Falk, H. Georgi, B. Grinstein, and M.B. Wise, Nucl. Phys. B **343**, 1 (1990).
23. A.F. Falk, B. Grinstein, and M.E. Luke, Nucl. Phys. B **357**, 185 (1991).

24. T. Mannel, W. Roberts, and Z. Ryzak, Nucl. Phys. B **368**, 204 (1992).
25. M. Neubert, Phys. Rep. **245**, 259 (1994).
26. H. Georgi, in: Perspectives in the Standard Model, Proceedings of the Theoretical Advanced Study Institute in Elementary Particle Physics (TASI-91), Boulder, Colorado, 1991, edited by R.K. Ellis, C.T. Hill, and J.D. Lykken (World Scientific, Singapore, 1992), p. 589.
27. B. Grinstein, in: High Energy Phenomenology, Proceedings of the Workshop on High Energy Phenomenology, Mexico City, Mexico, 1991, edited by M.A. Pérez and R. Huerta (World Scientific, Singapore, 1992), p. 161.
28. N. Isgur and M.B. Wise, in: Heavy Flavours, edited by A.J. Buras and M. Lindner (World Scientific, Singapore, 1992), p. 234.
29. T. Mannel, in: QCD-20 Years Later, Proceedings of the Workshop on QCD, Aachen, Germany, 1992, edited by P.M. Zerwas and H.A. Kastrup (World Scientific, Singapore, 1993), p. 634.
30. M. Shifman, Minneapolis preprint TPI-MINN-95/31-T (1995) [hep-ph/9510377], to appear in: QCD and Beyond, Proceedings of the Theoretical Advanced Study Institute in Elementary Particle Physics (TASI-95), Boulder, Colorado, 1995.
31. D.J. Gross and F. Wilczek, Phys. Rev. Lett. **30**, 1343 (1973).
32. H.D. Politzer, Phys. Rev. Lett. **30**, 1346 (1973).
33. T. Appelquist and H.D. Politzer, Phys. Rev. Lett. **34**, 43 (1975).
34. M.A. Shifman, A.I. Vainshtein, and V.I. Zakharov, Nucl. Phys. B **120**, 316 (1977).
35. E. Witten, Nucl. Phys. B **122**, 109 (1977).
36. J. Polchinski, Nucl. Phys. B **231**, 269 (1984).
37. K. Wilson, Phys. Rev. **179**, 1499 (1969); D **3**, 1818 (1971).
38. W. Zimmermann, Ann. Phys. **77**, 536 and 570 (1973).
39. G. Altarelli and L. Maiani, Phys. Lett. B **52**, 351 (1974).
40. M.K. Gaillard and B.W. Lee, Phys. Rev. Lett. **33**, 108 (1974).
41. F.J. Gilman and M.B. Wise, Phys. Rev. D **27**, 1128 (1983).
42. N. Isgur and M.B. Wise, Phys. Rev. Lett. **66**, 1130 (1991).
43. A.F. Falk, Nucl. Phys. B **378**, 79 (1992).
44. A.F. Falk, M. Neubert, and M.E. Luke, Nucl. Phys. B **388**, 363 (1992).
45. A.F. Falk and M. Neubert, Phys. Rev. D **47**, 2965 and 2982 (1993).
46. I.J. Kroll, preprint FERMILAB-CONF-96-032 (1996) [hep-ex/9602005], to appear in: Proceedings of the 17th International Symposium on Lepton Photon Interactions (LP95), Beijing, P.R. China, August 1995.
47. G. Apollinari (CDF Collaboration), presented at the Aspen Winter Conference on Particle Physics, Aspen, Colorado, January 1996 (URL: <http://www-cdf.fnal.gov/physics/new/bottom/cdf3352/>).
48. P. Ball and V.M. Braun, Phys. Rev. D **49**, 2472 (1994).
49. V. Eletsky and E. Shuryak, Phys. Lett. B **276**, 191 (1992).
50. M. Neubert, Phys. Lett. B **322**, 419 (1994).
51. M. Beneke and V.M. Braun, Nucl. Phys. B **426**, 301 (1994).
52. I.I. Bigi, M.A. Shifman, N.G. Uraltsev and A.I. Vainshtein, Phys. Rev. D **50**, 2234 (1994).
53. M. Neubert and V. Rieckert, Nucl. Phys. B **382**, 97 (1992).
54. M.E. Luke, Phys. Lett. B **252**, 447 (1990).
55. M. Ademollo and R. Gatto, Phys. Rev. Lett. **13**, 264 (1964).
56. M. Neubert, Nucl. Phys. B **416**, 786 (1994).
57. P. Cho and B. Grinstein, Phys. Lett. B **285**, 153 (1992).
58. M. Neubert, Phys. Lett. B **264**, 455 (1991).
59. G. Preparata and W.I. Weisberger, Phys. Rev. **175**, 1965 (1968).

60. H. Albrecht et al. (ARGUS Collaboration), *Z. Phys. C* **57**, 533 (1993).
61. B. Barish et al. (CLEO Collaboration), *Phys. Rev. D* **51**, 1041 (1995).
62. D. Buskulic et al. (ALEPH Collaboration), *Phys. Lett. B* **359**, 236 (1995).
63. P. Abreu et al. (DELPHI Collaboration), preprint CERN-PPE/96-11 (1996).
64. S. Stone, in: *Proceedings of the 8th Annual Meeting of the Division of Particles and Fields of the APS, Albuquerque, New Mexico, 1994*, edited by S. Seidel (World Scientific, Singapore, 1995), p. 871.
65. C.G. Boyd, B. Grinstein and R.F. Lebed, *Nucl. Phys. B* **461**, 493 (1996);
C.G. Boyd and R.F. Lebed, San Diego preprint UCSD/PTH 95-23 (1995) [hep-ph/9512363].
66. I. Caprini and M. Neubert, preprint CERN-TH/95-255 (1995) [hep-ph/9603414], to appear in *Phys. Lett. B*.
67. M. Neubert, *Nucl. Phys. B* **371**, 149 (1992).
68. S.J. Brodsky, G.P. Lepage, and P.B. Mackenzie, *Phys. Rev. D* **28**, 228 (1983);
G.P. Lepage and P.B. Mackenzie, *Phys. Rev. D* **48**, 2250 (1993).
69. M. Neubert, *Phys. Lett. B* **341**, 367 (1995).
70. X. Ji and M.J. Musolf, *Phys. Lett. B* **257**, 409 (1991).
71. D.J. Broadhurst and A.G. Grozin, *Phys. Lett. B* **267**, 105 (1991).
72. A.F. Falk and B. Grinstein, *Phys. Lett. B* **247**, 406 (1990).
73. M. Neubert, *Phys. Rev. D* **46**, 2212 (1992).
74. M. Neubert, *Phys. Rev. D* **51**, 5924 (1995).
75. A. Czarnecki, Karlsruhe preprint TTP 96-05 (1996) [hep-ph/9603261].
76. T. Mannel, *Phys. Rev. D* **50**, 428 (1994).
77. M. Shifman, N.G. Uraltsev, and A. Vainshtein, *Phys. Rev. D* **51**, 2217 (1995).
78. M. Neubert, *Phys. Lett. B* **338**, 84 (1994).
79. J.D. Bjorken, in: *Results and Perspectives in Particle Physics, Proceedings of the 4th Rencontres de Physique de la Vallée d'Aoste, La Thuile, Italy, 1990*, edited by M. Greco (Editions Frontières, Gif-sur-Yvette, 1990), p. 583; in: *Gauge Bosons and Heavy Quarks, Proceedings of the 18th SLAC Summer Institute on Particle Physics, Stanford, California, 1990*, edited by J.F. Hawthorne (SLAC Report No. 378, Stanford, 1991), p. 167.
80. N. Isgur and M.B. Wise, *Phys. Rev. D* **43**, 819 (1991).
81. J.D. Bjorken, I. Dunietz, and J. Taron, *Nucl. Phys. B* **371**, 111 (1992).
82. N. Isgur, M.B. Wise, and M. Youssefmir, *Phys. Lett. B* **254**, 215 (1991).
83. M.B. Voloshin, *Phys. Rev. D* **46**, 3062 (1992).
84. A.G. Grozin and G.P. Korchemsky, *Phys. Rev. D* **53**, 1378 (1996).
85. M. Neubert, in: *Electroweak Interactions and Unified Theories, Proceedings of the 30th Rencontres de Moriond, Les Arcs, France, March 1995*, edited by J. Trân Thanh Vân (Editions Frontières, Gif-sur-Yvette, 1995), p. 169;
G.P. Korchemsky and M. Neubert, in preparation.
86. E. Bagan, P. Ball, and P. Gosdzinsky, *Phys. Lett. B* **301**, 249 (1993).
87. M. Neubert, *Phys. Rev. D* **47**, 4063 (1993).
88. B. Blok and M. Shifman, *Phys. Rev. D* **47**, 2949 (1993).
89. S. Narison, *Phys. Lett. B* **325**, 197 (1994).
90. K.C. Bowler et al., *Phys. Rev. D* **52**, 5067 (1995).
91. M. Neubert, *Phys. Rev. D* **46**, 3914 (1992);
Z. Ligeti, Y. Nir, and M. Neubert, *ibid.* **49**, 1302 (1994).
92. J.E. Duboscq et al. (CLEO Collaboration), Cornell preprint CLNS 95/1372 (1995).
93. M. Neubert, *Phys. Rev. D* **46**, 1076 (1992).
94. E. Bagan, P. Ball, V.M. Braun, and H.G. Dosch, *Phys. Lett. B* **278**, 457 (1992).
95. A.F. Falk, M. Luke, and M.J. Savage, Toronto preprint UTPT-95-24 (1995) [hep-

- ph/9511454].
96. M. Gremm, A. Kapustin, Z. Ligeti, and M.B. Wise, Caltech preprint CALT-68-2043 (1996) [hep-ph/9603314].
 97. F.E. Close and A. Wambach, *Phys. Lett. B* **348**, 207 (1995).
 98. N. Isgur, D. Scora, B. Grinstein, and M.B. Wise, *Phys. Rev. D* **39**, 799 (1989).
 99. M. Wirbel, B. Stech, and M. Bauer, *Z. Phys. C* **29**, 637 (1985);
M. Bauer, B. Stech, and M. Wirbel, *ibid.* **34**, 103 (1987).
 100. S. Narison, *Phys. Lett. B* **283**, 384 (1992).
 101. P. Ball, *Phys. Rev. D* **48**, 3190 (1993).
 102. A. Khodjamirian and R. Rückl, *Nucl. Instr. and Meth. A* **368**, 28 (1995).
 103. D.R. Burford et al., *Nucl. Phys. B* **447**, 425 (1995).
 104. C.R. Allton et al., *Phys. Lett. B* **345**, 513 (1995).
 105. H-n. Li and H.-L. Yu, *Phys. Rev. Lett.* **74**, 4388 (1995).
 106. J.G. Körner and G.A. Schuler, *Z. Phys. C* **38**, 511 (1988).
 107. D. Scora and N. Isgur, *Phys. Rev. D* **52**, 2783 (1995).
 108. J.M. Flynn et al., *Nucl. Phys. B* **461**, 327 (1996).
 109. C.G. Boyd, B. Grinstein, and R.F. Lebed, *Phys. Rev. Lett.* **74**, 4603 (1995); *Phys. Lett. B* **353**, 306 (1995).
 110. L. Lellouch, Marseille preprint CPT-95-P-3236 (1995) [hep-ph/9509358].
 111. B. Stech, *Phys. Lett. B* **354**, 447 (1995).
 112. J. Chay, H. Georgi, and B. Grinstein, *Phys. Lett. B* **247**, 399 (1990).
 113. I.I. Bigi, N.G. Uraltsev, and A.I. Vainshtein, *Phys. Lett. B* **293**, 430 (1992) [E: **297**, 477 (1993)];
I.I. Bigi, M.A. Shifman, N.G. Uraltsev, and A.I. Vainshtein, *Phys. Rev. Lett.* **71**, 496 (1993);
I.I. Bigi et al., in: *Proceedings of the Annual Meeting of the Division of Particles and Fields of the APS, Batavia, Illinois, 1992*, edited by C. Albright et al. (World Scientific, Singapore, 1993), p. 610.
 114. B. Blok, L. Koyrakh, M.A. Shifman, and A.I. Vainshtein, *Phys. Rev. D* **49**, 3356 (1994) [E: **50**, 3572 (1994)].
 115. A.V. Manohar and M.B. Wise, *Phys. Rev. D* **49**, 1310 (1994).
 116. M. Luke and M.J. Savage, *Phys. Lett. B* **321**, 88 (1994);
A.F. Falk, M. Luke, and M.J. Savage, *Phys. Rev. D* **49**, 3367 (1994).
 117. T. Mannel, *Nucl. Phys. B* **413**, 396 (1994).
 118. A.F. Falk, Z. Ligeti, M. Neubert, and Y. Nir, *Phys. Lett. B* **326**, 145 (1994).
 119. M. Neubert, *Phys. Rev. D* **49**, 3392 and 4623 (1994).
 120. I.I. Bigi, M.A. Shifman, N.G. Uraltsev, and A.I. Vainshtein, *Int. J. Mod. Phys. A* **9**, 2467 (1994).
 121. E.C. Poggio, H.R. Quinn, and S. Weinberg, *Phys. Rev. D* **13**, 1958 (1976).
 122. M. Girone and M. Neubert, *Phys. Rev. Lett.* **76**, 3061 (1996).
 123. M. Shifman, Minneapolis preprint TPI-MINN-95/15-T (1995) [hep-ph/9505289], to appear in: *Proceedings of the Joint Meeting of the International Symposium on Particles, Strings and Cosmology and the 19th Johns Hopkins Workshop on Current Problems in Particle Theory, Baltimore, Maryland, March 1995*.
 124. G. Altarelli and L. Maiani, *Phys. Lett. B* **52**, 351 (1974).
 125. M.K. Gaillard and B.W. Lee, *Phys. Rev. Lett.* **33**, 108 (1974).
 126. F.G. Gilman and M.B. Wise, *Phys. Rev. D* **20**, 2392 (1979).
 127. G. Altarelli, G. Curci, G. Martinelli, and S. Petrarca, *Phys. Lett. B* **99**, 141 (1981); *Nucl. Phys. B* **187**, 461 (1981).
 128. A.J. Buras and P.H. Weisz, *Nucl. Phys. B* **333**, 66 (1990).
 129. Y. Nir, *Phys. Lett. B* **221**, 184 (1989).

130. M. Luke, M.J. Savage, and M.B. Wise, Phys. Lett. B **343**, 329 (1995); **345**, 301 (1995).
131. P. Ball and U. Nierste, Phys. Rev. D **50**, 5841 (1994).
132. P. Ball, M. Beneke, and V.M. Braun, Nucl. Phys. B **452**, 563 (1995); Phys. Rev. D **52**, 3929 (1995).
133. T. Skwarnicki, Syracuse preprint HEPHY-95-05 (1995) [hep-ph/9512395], to appear in: Proceedings of the 17th International Symposium on Lepton Photon Interactions (LP95), Beijing, P.R. China, August 1995.
134. P. Perret, Clermont-Ferrand preprint PCCF-RI 9507 (1995), to appear in: Proceedings of the International Europhysics Conference on High Energy Physics, Brussels, Belgium, September 1995.
135. T. Browder, Hawaii preprint UH 511-836-95 (1995) [hep-ex/9602009], to appear in: Proceedings of the International Europhysics Conference on High Energy Physics, Brussels, Belgium, September 1995.
136. G. Calderini, presented at the 31th Rencontres de Moriond: QCD and High Energy Hadronic Interactions, Les Arcs, France, March 1996.
137. G. Altarelli and S. Petrarca, Phys. Lett. B **261**, 303 (1991).
138. I. Bigi, B. Blok, M.A. Shifman, and A. Vainshtein, Phys. Lett. B **323**, 408 (1994).
139. E. Bagan, P. Ball, V.M. Braun, and P. Gosdzinsky, Nucl. Phys. B **432**, 3 (1994); Phys. Lett. B **342**, 362 (1995) [E: to appear in Phys. Lett. B];
E. Bagan, P. Ball, B. Fiol, and P. Gosdzinsky, Phys. Lett. B **351**, 546 (1995).
140. M. Neubert and C.T. Sachrajda, preprint CERN-TH/96-19 (1996) [hep-ph/9603202].
141. G. Buchalla, I. Dunietz, and H. Yamamoto, Phys. Lett. B **364**, 188 (1996).
142. I. Dunietz, P.S. Cooper, A.F. Falk, and M.B. Wise, Phys. Rev. Lett. **73**, 1075 (1994).
143. W.F. Palmer and B. Stech, Phys. Rev. D **48**, 4174 (1993).
144. A.F. Falk, M.B. Wise, and I. Dunietz, Phys. Rev. D **51**, 1183 (1995).
145. B. Blok and T. Mannel, Karlsruhe preprint TTP 95-22 (1995) [hep-ph/9505288].
146. C.G. Boyd, B. Grinstein, and A.V. Manohar, San Diego preprint UCSD-PTH-95-19 (1995) [hep-ph/9511233].
147. M. Neubert, preprint CERN-TH/95-307 (1995) [hep-ph/9511409], to appear in: Proceedings of the 17th International Symposium on Lepton Photon Interactions (LP95), Beijing, P.R. China, August 1995.
148. B. Grzadkowski and W.-S. Hou, Phys. Lett. B **272**, 383 (1991).
149. A.L. Kagan, Phys. Rev. D **51**, 6196 (1995).
150. L. Roszkowski and M. Shifman, Phys. Rev. D **53**, 404 (1996).
151. M. Ciuchini, E. Gabrielli, and G.F. Giudice, preprint CERN-TH/96-73 (1996).
152. The value of $\tau(\Lambda_b)/\tau(B^0)$ is obtained by averaging the result 0.76 ± 0.05 quoted in Ref.⁴⁶ with the new preliminary value $0.85 \pm 0.10 \pm 0.05$ reported in: G. Apollinari (CDF Collaboration), presented at the Aspen Winter Conference on Particle Physics, Aspen, Colorado, January 1996
(URL: <http://www-cdf.fnal.gov/physics/new/bottom/cdf3395/>).
153. I.I. Bigi et al., in: B Decays, edited by S. Stone, Second Edition (World Scientific, Singapore, 1994), p. 134;
For a recent review, see: I.I. Bigi, Notre Dame preprint UND-HEP-95-BIG02 (1995) [hep-ph/9508408].
154. B. Guberina, S. Nussinov, R. Peccei, and R. Rückl, Phys. Lett. B **89**, 111 (1979).
155. N. Bilic, B. Guberina, and J. Trampetic, Nucl. Phys. B **248**, 261 (1984);
B. Guberina, R. Rückl, and J. Trampetic, Z. Phys. C **33**, 297 (1986).
156. M. Shifman and M. Voloshin, Sov. J. Nucl. Phys. **41**, 120 (1985); JETP **64**, 698 (1986).
157. M.A. Shifman, A.I. Vainshtein, and V.I. Zakharov, Nucl. Phys. B **147**, 385 and 448 (1979).
158. V. Chernyak, Novosibirsk preprint BUDKERINP-94-69 (1994) [hep-ph/9407353].

159. J.L. Rosner, preprint CERN-TH/96-24 (1996) [hep-ph/9602265].
160. J.H. Christenson, J.W. Cronin, V.L. Fitch, and R. Turlay, *Phys. Rev. Lett.* **13**, 138 (1964).
161. A.D. Sakharov, *ZhETF Pis. Red.* **5**, 32 (1967); *JETP Lett.* **5**, 24 (1967).
162. V. Baluni, *Phys. Rev. D* **19**, 2227 (1979).
163. R.J. Crewther, P. Di Vecchia, G. Veneziano, and E. Witten, *Phys. Lett. B* **88**, 123 (1979) [E: **91**, 487 (1980)].
164. R.D. Peccei and H.R. Quinn, *Phys. Rev. Lett.* **38**, 1440 (1977); *Phys. Rev. D* **16**, 1791 (1977).
165. Y. Nir, in: *The Third Family and the Physics of Flavour*, Proceedings of the 20th SLAC Summer Institute on Particle Physics, Stanford, California, 1992, edited by L. Vassilian (SLAC Report No. 412, Stanford, 1993), p. 81;
Y. Nir and H.R. Quinn, *Annu. Rev. Nucl. Part. Sci.* **42**, 221 (1992).
166. G. Buchalla, A.J. Buras, and M.E. Lautenbacher, Munich preprint MPI-Ph/95-104 (1995) [hep-ph/9512380], to appear in *Rev. Mod. Phys.*
167. M. Bander, D. Silverman, and A. Soni, *Phys. Rev. Lett.* **43**, 242 (1979).
168. M. Gronau and D. London, *Phys. Rev. Lett.* **65**, 3381 (1990); *Phys. Lett. B* **253**, 483 (1991).
169. Y. Nir and H.R. Quinn, *Phys. Rev. D* **42**, 1473 (1990); *Phys. Rev. Lett.* **67**, 541 (1991).
170. H.J. Lipkin, Y. Nir, H.R. Quinn, and A. Snyder, *Phys. Rev. D* **44**, 1454 (1991).
171. M. Gronau and D. Wyler, *Phys. Lett. B* **265**, 172 (1991).
172. M. Gronau, J.L. Rosner, and D. London, *Phys. Rev. Lett.* **73**, 21 (1994);
M. Gronau, O.F. Hernández, D. London, and J.L. Rosner, *Phys. Rev. D* **50**, 4529 (1994);
O.F. Hernández, D. London, M. Gronau, and J.L. Rosner, *Phys. Lett. B* **333**, 500 (1994).
173. R. Aleksan, to appear in: *Proceedings of the International Europhysics Conference on High Energy Physics*, Brussels, Belgium, September 1995.
174. A.B. Carter and A.I. Sanda, *Phys. Rev. Lett.* **45**, 952 (1980); *Phys. Rev. D* **23**, 1567 (1981).
175. I.I. Bigi and A.I. Sanda, *Nucl. Phys. B* **193**, 85 (1981); **281**, 41 (1987).
176. I. Dunietz and J.L. Rosner, *Phys. Rev. D* **34**, 1404 (1986).
177. N. Cabibbo, *Phys. Rev. Lett.* **10**, 531 (1963).
178. M. Kobayashi and K. Maskawa, *Prog. Theor. Phys.* **49**, 652 (1973).
179. C. Jarlskog, in: *CP Violation*, edited by C. Jarlskog (World Scientific, Singapore, 1989), p. 3.
180. C. Jarlskog, *Phys. Rev. Lett.* **55**, 1039 (1985); *Z. Phys. C* **29**, 491 (1985).
181. L.L. Chau and W.-Y. Keung, *Phys. Rev. Lett.* **53**, 1802 (1984).
182. L. Wolfenstein, *Phys. Rev. Lett.* **51**, 1945 (1983).
183. J.D. Bjorken, presented in discussions at the Workshop on Experiments, Detectors and Experimental Areas for the Supercollider, Berkeley, California, July 1987 (Proceedings edited by R. Donaldson and M.G.D. Gilchriese, World Scientific, Singapore, 1988).
184. C. Jarlskog and R. Stora, *Phys. Lett. B* **208**, 268 (1988).
185. I.I. Bigi, V.A. Khoze, N.G. Uraltsev, and A.I. Sanda, in: *CP Violation*, edited by C. Jarlskog (World Scientific, Singapore, 1989), p. 175.
186. C.O. Dib, I. Dunietz, F.J. Gilman, and Y. Nir, *Phys. Rev. D* **41**, 1522 (1990);
F.J. Gilman and Y. Nir, *Annu. Rev. Nucl. Part. Sci.* **40**, 213 (1990).
187. C.S. Kim, J.L. Rosner, and S.-P. Yuan, *Phys. Rev. D* **42**, 96 (1990).
188. M. Schmidtler and K.R. Schubert, *Z. Phys. C* **53**, 347 (1992).
189. M. Lusignoli, L. Maiani, G. Martinelli, and L. Reina, *Nucl. Phys. B* **369**, 139 (1992).
190. G.R. Harris and J.L. Rosner, *Phys. Rev. D* **45**, 946 (1992).

191. A.J. Buras, M.E. Lautenbacher, and G. Ostermayer, *Phys. Rev. D* **50**, 3433 (1994).
192. A.J. Buras, M. Jamin, and P.H. Weisz, *Nucl. Phys. B* **347**, 491 (1990).
193. T. Inami and C.S. Lim, *Progr. Theor. Phys.* **65**, 297 and 1772 (1981).
194. A.J. Buras, *Phys. Rev. Lett.* **46**, 1354 (1981).
195. M. Neubert, *Phys. Rev. D* **45**, 2451 (1992).
196. C.T. Sachrajda, in: *B Decays*, edited by S. Stone, Second Edition (World Scientific, Singapore, 1994), p. 602.
197. A. Duncan et al., *Phys. Rev. D* **51**, 5101 (1995).
198. C.W. Bernard, J.N. Labrenz, and A. Soni, *Phys. Rev. D* **49**, 2536 (1994).
199. T. Draper and C. McNeile, *Nucl. Phys. B (Proc. Suppl.)* **34**, 453 (1994).
200. A. Abada et al., *Nucl. Phys. B* **376**, 172 (1992).
201. A.J. Buras and M.K. Harlander, in: *Heavy Flavours*, edited by A.J. Buras and M. Lindner (World Scientific, Singapore, 1992), p. 58;
A.J. Buras, *Nucl. Instr. and Meth. A* **368**, 1 (1995);
G. Buchalla, A.J. Buras, and M.K. Harlander, *Nucl. Phys. B* **349**, 1 (1991).
202. S. Sharpe, *Nucl. Phys. B (Proc. Suppl.)* **34**, 403 (1994).
203. N. Ishizuka et al., *Phys. Rev. Lett.* **71**, 24 (1993).
204. W.A. Bardeen, A.J. Buras, and J.-M. Gérard, *Phys. Lett. B* **211**, 343 (1988);
J.-M. Gérard, *Acta Phys. Pol. B* **21**, 257 (1990).
205. J. Bijnens and J. Prades, *Nucl. Phys. B* **444**, 523 (1995).
206. J.F. Donoghue, E. Golowich, and B.R. Holstein, *Phys. Lett. B* **119**, 412 (1982).
207. A. Pich and E. de Rafael, *Phys. Lett. B* **158**, 477 (1985); *Nucl. Phys. B* **358**, 311 (1991);
J. Prades et al., *Z. Phys. C* **51**, 287 (1991).
208. G.D. Barr et al. (NA31 Collaboration), *Phys. Lett. B* **317**, 233 (1993).
209. L.K. Gibbons et al. (E731 Collaboration), *Phys. Rev. Lett.* **70**, 1203 (1993).
210. G. Buchalla, A.J. Buras, and M.K. Harlander, *Nucl. Phys. B* **337**, 313 (1990).
211. A.J. Buras, M. Jamin, and M.E. Lautenbacher, *Nucl. Phys. B* **408**, 209 (1993).
212. M. Ciuchini et al., *Z. Phys. C* **68**, 239 (1995).
213. D. London and R.D. Peccei, *Phys. Lett. B* **223**, 257 (1989).
214. M. Gronau, *Phys. Rev. Lett.* **63**, 1451 (1989).
215. B. Grinstein, *Phys. Lett. B* **229**, 280 (1989).